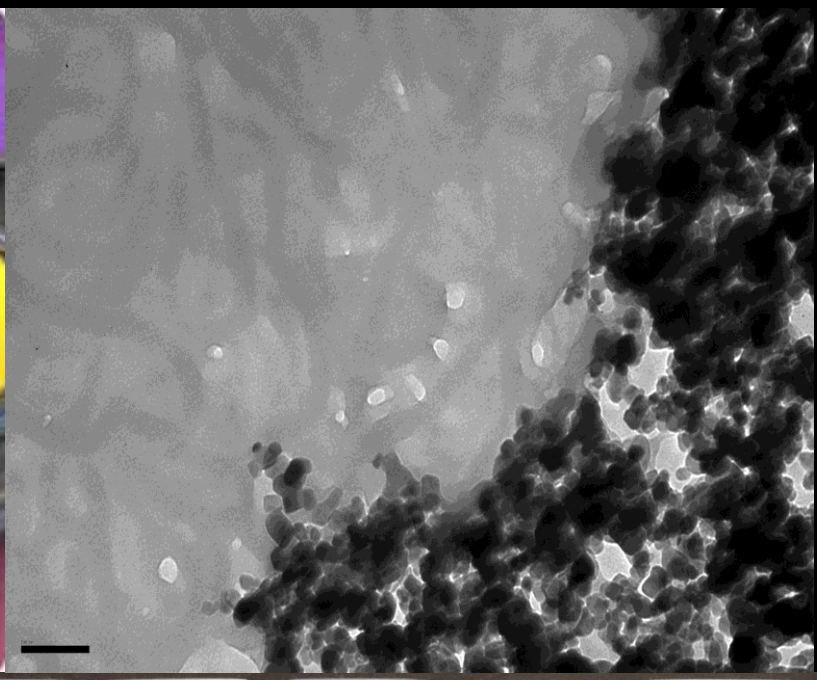

João Ricardo Carapito Gonçalves da Costa

Development of block copolymers for advanced coatings applications

Thesis Project in the scientific area of Chemical Engineering, supervised by Professor Jorge Coelho and submitted to the Department of Chemical Engineering, Faculty of Science and Technology, University of Coimbra

September 2014

· U C ·

Universidade de Coimbra

João Ricardo Carapito Gonçalves da Costa

Development of block copolymers for advanced coatings applications

Thesis Project in the scientific area of Chemical Engineering, supervised by Professor Jorge Coelho and submitted to the Department of Chemical Engineering, Faculty of Science and Technology, University of Coimbra

Supervisor(s):

Prof. Dr. Jorge Coelho

Dr. Nuno Rocha

Coimbra

2014

· U C ·

UNIVERSIDADE DE COIMBRA

“The mind that opens to a new idea

never returns to its original size.”

ALBERT EINSTEIN

Acknowledgements

Em primeiro lugar gostaria de agradecer aos meus orientadores, Prof. Dr. Jorge Coelho e Dr. Nuno Rocha, pela orientação prestada que foi fundamental para ultrapassar os diversos obstáculos que surgiram, pelo encorajamento e motivação muito importantes para atingir os meus objetivos, mesmo nos momentos mais difíceis, e também pelos conhecimentos científicos que me transmitiram e permitiram acabar esta etapa com um sentimento de satisfação por tudo o que consegui aprender com eles. Também agradeço o exemplo de profissionalismo demonstrado, a disponibilidade mostrada, em especial ao Prof. Dr. Jorge Coelho, que mesmo em tempo de férias se prontificou para me ajudar, e por terem contribuído para a evolução do meu caráter a nível profissional e fomentado espírito crítico.

Gostaria também de agradecer em geral às pessoas que pertenceram ao grupo de investigação de polímeros, em particular as presentes no laboratório B37, durante o desenvolvimento do meu trabalho, pois também elas ajudaram durante a minha jornada, quer no manuseamento de equipamentos, esclarecimento de dúvidas, quer também nos momentos de descontração, que na altura certa são uma lufada de ar fresco, fazendo-nos avançar com uma energia renovada. Agradeço em especial ao Dr. Arménio e Joana Mendes, pois foi graças à sua ajuda que foi possível contornar a maior parte dos problemas verificados durante as reações de hidrólise. Agradeço também à Joana Góis pelo acompanhamento durante as medições de DLS e potencial zeta, durante as várias semanas, pois por vezes precisou de colocar o seu trabalho de parte para que eu pudesse realizar as medições, e agradeço-lhe também pelos concelhos que me ajudaram a avançar mais depressa. Em especial um obrigado à Daniela Rodrigues que me acompanhou desde o início, ajudando nas mais variadas tarefas laboratoriais e no planeamento do tempo, para que fosse possível realizar as tarefas propostas. Agradeço também a amizade demostrada que foi muito importante nas etapas mais complicadas deste projeto.

Agradeço também ao Dr. Sérgio Silva do Departamento de Química pela disponibilidade e auxílio no manuseamento do reómetro.

Ao Eng.º Jorge Moniz da Resiquímica, pela disponibilidade para experimentar alguns dos copolímeros numa formulação para tintas, e por me ter transmitido conhecimentos acerca desta área, que apresenta variados pormenores que passam despercebidos à maioria das pessoas.

Agradeço ao Prof. Dr. Fernão Magalhães e Sandra Monteiro da Universidade do Porto, por me terem orientado e explicado vários aspetos relacionados com as partículas de dióxido de titânio, como alguns dos testes usados para verificar a boa dispersão destas partículas, quando estas possuem uma dimensão nanométrica.

Um obrigado aos meus amigos que estiveram sempre do meu lado durante esta caminhada, pelo companheirismo, força e apoio mesmo nos momentos mais difíceis, pois foi em grande parte graças a eles que foi possível continuar e concluir mais esta etapa.

Por último, mas não menos importante, dirijo o meu agradecimento especial à minha família, pelo seu apoio incondicional, incentivo, amizade e paciência nos momentos em que as coisas não corriam como desejado. Também agradeço por nunca terem deixado de acreditar no meu sucesso, meu quando eu próprio não estava tão convicto disso.

Abstract

The objective of this work concerned the synthesis, characterize and evaluate the capability of some block copolymers, constituted by a hydrophilic and a hydrophobic segment of different amphiphilic block copolymers designed to stabilize and disperse, to form micelles around TiO_2 particles in order to stabilize and disperse them in a water-based paint. This has the purpose to find a better dispersant for TiO_2 particles than the commercial dispersant used, providing better brightness to the paint and with that, reduce the amount of titania used, since is an expensive raw material.

The synthesis of the block copolymers was performed using an ATRP method. The new structures were characterized by GPC, to determine the molecular weight and polydispersity, and by NMR, to calculate the monomers conversion, the monomers repeating units and to determine the percentage of hydrolysis from the PtBA group into PAA group. The stabilization and dispersing capacity from the synthesized copolymers were analyzed by DLS, zeta potential and viscosity measurements.

The results revealed that PAA_{26}-*b*-$P4VP_{30}$ and PAA_{41}-*b*-$PDMAEMA_{56}$ provided better stabilization, with little variations in hydrodynamic diameters through 12 days, and presented the stronger electrostatic repulsion among the copolymers studied. Contrarily, the samples of $mPEG_{113}$-*b*-$PDMAEMA_{44}$ and $mPEG_{45}$-*b*-$PDMAEMA_{38}$ showed an opposite effect, instead of disperse TiO_2 particles, the copolymer seemed to act as a precipitating agent, probably due to bridging flocculation.

Three copolymers were analyzed in a paint formulation, through their CIELab parameters, brightness, contrast ratio, and storage stability at 50ºC, where viscosity were measured at the initial state, after 14 days and then at the 28^{th} day. $mPEG_{45}$-*b*-$P4VP_{40}$ sample presented a better value of brightness than $mPEG_{113}$-*b*-$P4VP_{34}$, which can be an indicator that hydrophilic segment (mPEG) needs to be long enough to avoid particles aggregation, and small enough to allow particles come closer each other. Also, it allows to presence of more particles per area unit, leading to higher brightness.

Contents

List of Tables

List of Figures

List of Abbreviations and Terms

ς	Zeta
^{1}H-NMR	Hydrogen-1 nuclear Magnetic Resonance
2VP	2-Vinylpyridine
4VP	4-Vinylpyridine
Al_2O_3	Aluminum oxide
ATRP	Atom transfer radical polymerization
BBiB	2-Bromoisobutyryl bromide
$CDCl_3$	Deuterated chloroform
$CHCl_3$	Chloroform
CLRP	Controlled/"living" radical polymerization
CMC	Critical micelle concentration
Co	Cobalt
CPC	2-Chloropropionyl chloride
Cu	Copper
CuBr	Copper (I) bromide
$CuBr_2$	Copper (II) bromide
$CuCl_2$	Copper(II) chloride
Đ	Polydispersity
D_2O	Deuterium oxide
Da	Dalton
DCM	Dichloromethane
D_h	Hydrodynamic diameter
DLS	Dynamic light scattering
DMAEMA	2-(Dimethylamino)ethyl methacrylate

DMAP	4-Dimethylaminopyridine
DMF	Dimethylformamide
DMSO	Dimethyl sulfoxide
DP	Degree of polymerization
Fe	Iron
GPC	Gel permeation chromatography
h	Hours
HCl	Chloridric acid
HPSEC	High performance size-exclusion chromatography
IPA	Isopropanol
L	Liter
LiBr	Lithium bromide
M	Molar
MANa	Sodium methacrylate
MBP	Methyl 2-bromopropionate
MeOH	Methanol
Me6TREN	Tris(2-dimethylaminoethyl)amine
mg	Milligrams
min	Minutes
mm	Millimeter
mmol	Millimole
Mo	Molybdenum
Mw	Molecular weight
mPEG	Poly(ethylene glycol) methyl ether
NaPAA	Sodium polyacrylate
N_2	Nitrogen

NaOH	Sodium hydroxide
Ni	Nickel
nm	Nanometer
NMP	Nitroxide-mediated polymerization
Os	Osmium
P_4VP	Poly(4-vinyl pyridine)
Pa	Pascal
PAA	Poly(acrylic acid)
Pd	Palladium
PDMAEMA	Poly(2-(dimethylamino)ethyl methacrylate)
PDI	Polydispersity index
PMDETA	N,N,N',N',N''-pentamethyldiethylenetriamine
PMMA	Poly(methyl methacrylate)
PtBA	Poly-(*tert*-butyl acrylate)
PTFE	Polytetrafluoroethylene
RAFT	Reversible addition fragmentation chain transfer polymerization
Re	Rhenium
RI	Refractive index
Ru	Ruthenium
SiO_2	Silicon dioxide
tBA	*Tert*-butyl acrylate
TEA	Triethylamine
TFA	Trifluoroacetic acid
THF	Tetrahydrofuran
Ti	Titanium
TiO_2	Titanium dioxide

TMS	Tetramethylsilane
μL	Microliter

1. General Introduction

1.1. The Project Aims

Titanium dioxide (TiO_2) is broadly used in several types of markets, such as paints, papermaking, papermaking, pharmaceutical industries, among others, due to its notable physicochemical properties. Those include be regarded as completely nontoxic and thermodynamically stable. However, the paint industry is the biggest market, representing nearly 60% of its global consumption. TiO_2 is the most expensive compound for a variety of paints, but its use ensures better paint properties, such as gloss, hiding power and allows to prepare particles with a relatively narrow particle size distribution, unlike other inorganic pigments (Farrokhpay 2009).

In the last years associated to the technological development, scientific knowledge and environmental concerns, the health and environmental hazards represented by using organic solvents in paints formulations have been focused of particular attention. This concern originated regulations to restrict the use of organic solvents in paint formulations, leading to the rapid development of water-based paints (Herbst and Hunger 2006). The appearance of water-based paints and restrictions to the use of organic solvents, turned the problem of dispersing and stabilize of TiO_2 particles in paints formulation a critical issue, since the TiO_2 is water insoluble. Considering that TiO_2 is the best known white pigment, it becomes critical to overcome the solubility problem, which causes flocculation of this pigment particles, causing a deterioration of its properties, such as gloss, when compared with well dispersed particles.

A first step to improve TiO_2 stability was made, through a surface coating treatment applied after its manufacture. This treatment consists in the coating of TiO_2 surface with inorganic oxides such as alumina, silica or zirconium, and with a final treatment of alumina, providing a better particle dispersion by decreasing the effect of Van der Waals attractive forces (Farrokhpay 2009). Despite the stabilization provided by this surface treatment, it stills inefficient and flocculation occurs. However, the final surface treatment with alumina has been shown to supply a strong adsorption by polymers, which allowed using them as dispersants of these particles (Farrokhpay 2009).

The purpose of this thesis consisted on the design of new dispersants for TiO_2 with better performance compared to the commercial products, namely Additol VXW 6200 which

is an acrylic copolymer, and was used as reference in this thesis. In a paint formulation, a better dispersion of TiO_2 particles makes the paint with higher values of gloss. A better dispersion allows also the reduction of the amount of the required TiO_2, which represents a significant cost reduction since TiO_2 is one of the most expensive raw materials from paint formulations.

To achieve proposed goal, the pathway chosen was the synthesis of some block copolymers with two segments, one hydrophilic, which is water soluble, and a hydrophobic segment to adsorb into particles surface, providing a barrier to stabilize the particles and prevent flocculation.

The copolymers were synthesized using an Atom Transfer Radical Polymerization (ATRP) method. It is a simple and efficient method that has demonstrated its feasibility to prepare polymers of predictable molecular weight, narrow molecular weight distribution and containing active chain ends that can be used to prepared block copolymers or further modification.

The expected result is the formation of micelle structures in the aqueous medium, since block copolymers are constituted by a hydrophilic and a hydrophobic segment, with a core constituted by the hydrophobic segment and the corona constituted by hydrophilic segment. It is expectable that the formation of these structures will take place around titania particles, through interactions between the hydrophobic segment and the titania surface, by means of hydrogen bonds of the hydrogens from hydrophobic segment and the hydrogen of Al-OH, on the particles surface, that was provided by the surface treatment that the particles were subjected.

1.2. Thesis Scope

This thesis is organized in 7 chapters and an Appendix section, which provides supplementary information to assist the results comprehension.

A comprehensive review in Chapter 2 discusses specific issues to better understand the method in this project, the need to develop better dispersants for TiO_2 particles in water-based paints and also the main characteristics of these particles.

Chapter 3 describes the experimental methods used to synthesize and characterize the block copolymers used. The characterization of copolymers is included and explained in the main body of Chapter 3, and supplementary data are provided in the Appendixes.

Chapter 4 describes the results obtained for the copolymers used regarding the stabilization and dispersion of TiO_2 particles in an aqueous medium, and a discussion about obtained results.

Finally, the main conclusions are summarized in Chapter 5, while Chapter 6 presents recommendations and suggestions for further work, and Chapter 7 presents the bibliography used.

2. Literature Review

2.1. Introduction

Nowadays, we live in a colorful world where paints, coatings and pigments play an important role in the society. The word pigment refers to small particles which can be inorganic or organic, colored, white, black or fluorescent, that are practically insoluble in the medium in which it is incorporated and are used on account of its coloring, protective or magnetic properties (Lambourne and Strivens 1999; Buxbaum and Pfaff 2005).

Despite dyes and pigments may be synonyms and are included in the general term "coloring materials", which denotes all materials used for their coloring properties (Buxbaum and Pfaff 2005), their scientific and industrial use is distinguished, according on their physical properties. In fact, in several cases the generic chemical structure of pigments and dyes is the same. Both are frequently similar as far as the basic chemical composition goes, and one structural skeleton may function either as a dye or as a pigment. The main difference between these two substances concerns to the fact of the dyes dissolve during their application and in the process, they lost the crystal or particulate structure, unlike pigments (Herbst and Hunger 2006). In turn, pigments are usually dispersed in vehicles or substrates for application, as for instance in the manufacture of inks, paints, plastics or other polymeric materials, and they retain a crystal or particulate structure throughout the coloration process (Lambourne and Strivens 1999).

Currently, there are many types of pigments available that can be used for the most different applications, but most of these pigments are used to provide a visual effect, mainly color and opacity (Lambourne and Strivens 1999).

The color of a pigment is mostly dependent on its chemical structure. The color stimulus consists of electromagnetic radiation in the range of wavelengths between about 400 nm and about 700 nm, usually denominated by light, that focuses on the eyes from the objects (Herbst and Hunger 2006). The selective absorption and reflection of various wavelengths of light that focus on the pigmented surface determines its hue (whether it is red or yellow, etc.). For example, a blue pigment has this appearance because it reflects the blue wavelengths of the incident white light that focus upon it and absorbs all of the other wavelengths. Hence, a blue car in orange sodium light looks black, and not blue because sodium light contains virtually no blue component (Lambourne and Strivens 1999).

Another two important factors, which determines the pigment color, are their crystal structure and particle size. Several pigments can exist in more than one crystal form, a property known as polymorphism, and these forms can be of very different colors. In terms of the particle size, the pigments composed for smaller particles are usually brighter in shade and change the hue of the pigment (Lambourne and Strivens 1999). Indeed, the pigments are made to have an optimal particle size leading to a maximum hiding power and color strength (Schmitz, Frommelius et al. 1999).

The hiding power refers to the ability of a layer of pigment medium to conceal previous substrate coloration turning it invisible. It is defined as the area over which a certain amount of a certain type of pigmented paint can be spread without losing its opacity. In another hand, it is also possible classify the hiding power as the minimum thickness of a layer which is necessary to conceal a given substrate. For that happen, the layer that conceals its substrate must scatter the light. The necessary amount of scattering will depend on the layer's thickness, the absorption of light within the layer, and the magnitude of the color differences of the substrate (Herbst and Hunger 2006). A less absorbing paint or a larger color differences of the substrate will lead to a higher scattering power needed to adequately hide the substrate. The hiding power also depends of the wavelength of the incident radiation. The hiding power of a pigmented layer is usually determined by applying it to a substrate with differently colored patches. Often black stripes are used on a white background or a black/white or grey/brown checkerboard surface with a standardized reflectance (e.g., R=80% for white and R=5% for black) (Herbst and Hunger 2006). For the quantification of a specific hiding power of a layer in relation to a standardized substrate, the maximum area may be specified over which the test paint can be spread without the loss of its opacity. Alternatively, it is also possible quantify the hiding power by finding the minimum thickness of layer that just effectively hides to the eye any difference in color between the differently colored patches of substrate surface (Herbst and Hunger 2006).

The world's production of inorganic pigments in 2000 was ca. 5.9×10^6 t, distributed by the following pigments (Buxbaum and Pfaff 2005):

Titanium dioxide 69%

Synthetic iron oxides 14%

Lithopone 3.5%

Zinc oxide 1%

Effect pigments 1%

Chromates <1%

Chromium oxide 0.5%

Mixed metal oxide pigments <0.5%

Ultramarine <0.5%

Iron blue <0.5%

The TiO_2 pigment, belonging to the group of white pigments, is used not only for white coloring and covering, but also for reducing colored and black pigments (Buxbaum and Pfaff 2005). Presently, the titania pigment is broadly used in paint, papermaking, plastic, cosmetic and pharmaceutical industries due to its outstanding physicochemical properties, but the paint industry represents nearly 60% of the global pigment consumption (Farrokhpay 2009). TiO_2 is the most expensive and indispensable compound for a variety of paints due to its high refractive index and inertness. Because of that, the homogeneous dispersion of TiO_2 in paints is a critical stage in the paints production, affecting the paint properties such as gloss, hiding power and color (Farrokhpay 2009).

The incomplete dispersion of the TiO_2 pigment particles jeopardizes the paints properties, involving the appearance of uneven coloring, the impossibility of achieve an optimum effect of the pigments, and higher cost of the formulation due to the necessity of using higher quantities of TiO_2. (Farrokhpay 2009; Karakas and Celik 2013). Unfortunately, during transportation and storage the so called primary particles build up to form agglomerates and aggregates, being necessary and important in the process of paint production the breakdown of these structures back into fine particles and its stabilization in this state (Schmitz, Frommelius et al. 1999). Therefore, the stabilization of TiO_2 particles is crucial in order to prevent re-agglomeration and to maximize the effect of TiO_2 in paint formulations. Therefore, the stabilization of TiO_2 is an essential key issue for its efficient use (Karakas and Celik 2013), and for this purpose dispersing agents are used, commonly known as dispersants (Schmitz, Frommelius et al. 1999).

It has become evident, in the recent years, that many of the solvents commonly used represent a health hazard, and legislation has been introduced to control their use. Even for solvents that have low toxicity, their odor may be unacceptable both in the working environment, near the manufacturing sites and user plants (Lambourne and Strivens 1999). With the increasing health and environmental concerns, regulations have been developed to

restrict the use of organic solvents in paint formulations, conducting to the rapid development of water-based products (Herbst and Hunger 2006).

In the solvent-based dispersions used in the paints formulation, nonionic surfactants are used, and the repulsive forces of an osmotic origin stabilize the pigments. Indeed, when two pigment particles approach each other to the point where the lipophilic tails of the adsorbed dispersant start to interpenetrate or to be compressed, the solvent diffuses into this very local region of an increase free energy of mixing and repels these particles from each other (Creutz, Jerome et al. 1998). In this case, a steric barrier prevents re-agglomeration (Schmitz, Frommelius et al. 1999).

In water-borne systems an ionic mechanism of electrostatic repulsion to disperse TiO_2 particles is required. In the architectural latex paints, by far the largest area of water-based paints, the electrostatic repulsion is provided by anionic dispersing agents like polyacrylic acid, widely used (Schmitz, Frommelius et al. 1999). However, with very strong environmental concerns opening an avenue to the use of aqueous dispersions at the expense of formerly used non-aqueous ones, the process of complete dispersion of pigments became in water-based paints essential. (Creutz and Jérôme 1999; Farrokhpay 2009). This thesis aims is the study of designed diblock copolymers as TiO_2 dispersant in water-based paints. An improved TiO_2 dispersion and stabilization allows a lesser formation of aggregates, which provides superior properties to the paints, such as gloss, color distribution and storage stability. Consequently, inferior quantities of TiO_2 will be required representing important cost savings for the industry.

2.2. Block Copolymers

Presently polymers are extremely useful to humankind, whether as natural or synthetic polymers. Indeed, natural polymers such as silk, wool, and cotton have been used for thousands of years, and synthetic polymers, are broadly used either as thermoplastics or thermosets. (Kumar and Gupta 2003).

Polymers are very long chain macromolecules in which hundreds or thousands of atoms are linked together, forming a one-dimensional array (Cincinnati, University et al. 2005). These macromolecules can have a very high molecular weight, and they usually consist of structural units bound together by covalent bonds (Kumar and Gupta 2003). These structural

units are a simply small molecule that repeats along the chain, being that molecule known as the repeating unit (Cincinnati, University et al. 2005). The polymers are obtained through the polymerization of the repeating units, called monomers, where monomer is repeated *n* times in the polymer structure (Kumar and Gupta 2003). In order to form polymers, the monomers either have reactive functional groups or double or triple bonds to provide the necessary linkages between the repeating units in the reaction (Kumar and Gupta 2003). When the reaction ends, the polymer has *n* repetition units in its backbone. This *n* is known as the degree of polymerization (DP) and it specifies the length of the polymer molecule (Ebewele 2000).

Polymerization occurs by the sequential reactions of monomers, and if the resulting polymer consists of a single type of monomer is called a homopolymer (Teraoka 2002). On the other hand, polymer molecules that composed of more than one kind of monomers are denominated by copolymers. Monomers composing the copolymer chain may be arranged in several degrees of order along the backbone, being even possible to have branches of a determined monomer in another type of backbone (Ebewele 2000).

Due to this degree of freedom, copolymers have different designations, such as schematized in Figure 1.

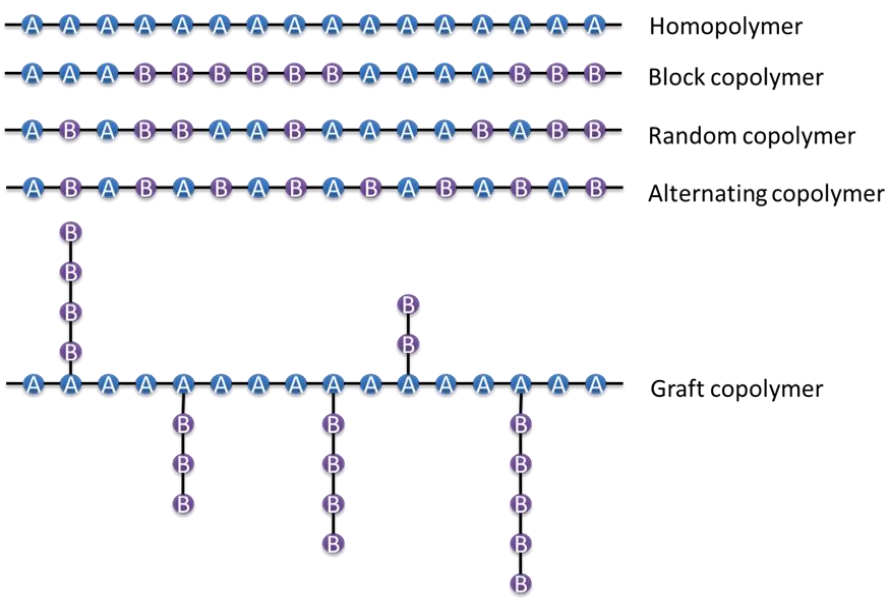

Figure 1 – Schematic representation of various copolymers systems (Stevens 1999).

Polymers can also exhibit very different types of architectures (Figure 2).

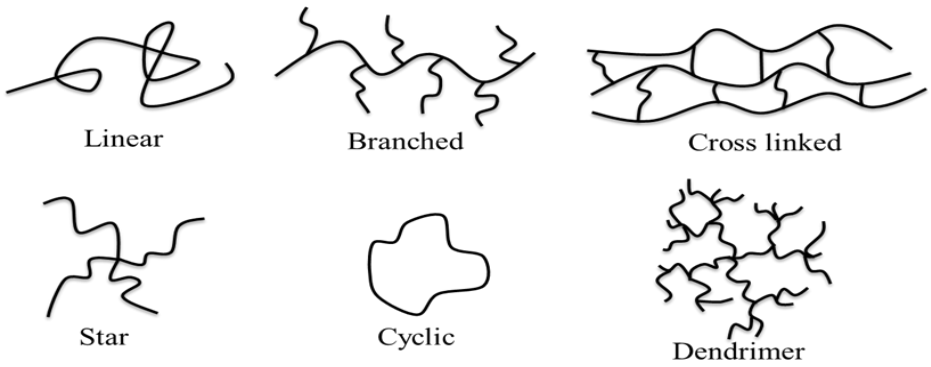

Figure 2 – Representation of polymer architectures (Hamley 2004; Lazzari, Liu et al. 2007).

Depending on the structure, architecture and type of bonds, polymers will show different physical properties. A crosslinking polymer is one example of this phenomenon, once that characteristic makes the polymer insoluble and with improved mechanical properties. (Mulder 1996).

The focus of attention in this work is the design of linear block copolymers, with different chains size, formed by two different segments that were selected to allow the dispersion and stabilization of the TiO_2 particles in aqueous medium. Along the work a standard notation for block copolymers, that is becoming accepted, is X-b-Y who denotes a diblock copolymer of polymer X and polymer Y, being that *b* can be replaced by the full term *block*, or the term can be omitted and the diblock denoted by X-Y (Hamley 2004). The copolymers used are mainly amphiphilic, meaning that they are composed by a water-soluble block (hydrophilic block) and by other block, which is not soluble (hydrophobic block).

Hydrophilic block is used in first place, in order to allow a good aqueous dispersion of TiO_2 particles besides offer a barrier to stabilize them, while hydrophobic block has the function of encompass the TiO_2 particles offering a physical barrier to prevent aggregation and posterior sedimentation. This subject will be discussed later in more detail.

2.3. Controlled reversible-deactivation radical polymerization

The synthesis task of block copolymers can be achieved through a few techniques such as step-growth polymerization, chain-growth polymerization and several techniques that belong to the controlled/"living" radical polymerization (CLRP) methods.

Briefly, in the step-growth polymerization, the polymer chain growth occurs by the reaction between reactive functional groups on end of the molecules. Since each molecule has at least one functional group, the reaction can take place between any two molecules, and these molecules can react at any time leading to a larger molecule (Ebewele 2000; Kumar and Gupta 2003).

On the other hand, the chain-growth polymerization occurs in presence of initiators that generates growth centers in the reaction medium, where monomer molecules are sequentially added (Kumar and Gupta 2003). For this kind of polymerization exists a variety of initiators that can be either ionic (cationic or anionic), free radical or complex coordination compounds (Stevens 1999). An example of a radicalar polymerization is schematized in Figure 3.

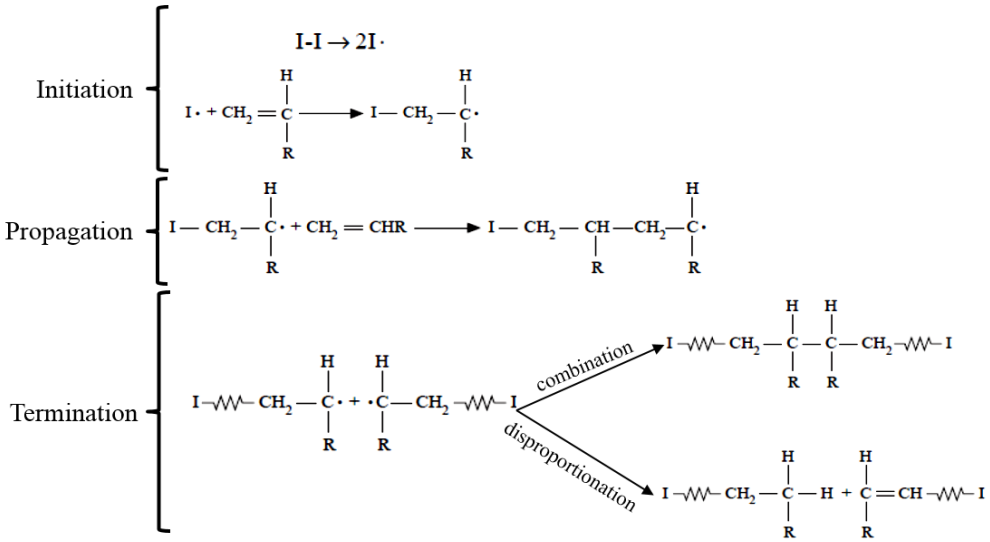

Figure 3 – Fundamental steps of chain-growth reaction (Ebewele 2000).

Both the step-growth and at chain-growth polymerization are not proper choices to produce controlled block copolymers. In the step-growth reaction, the monomer is consumed rapidly (Stevens 1999), since any two molecules can react each other, not being an interesting route to produce block copolymers with a controlled chain length. Unlike step-growth

reaction, the monomer is consumed relatively slowly in the chain-growth reaction, but in this case usually chain-terminating steps are involved (Stevens 1999). The anionic and cationic is not compatible to several monomer functionalities. Regarding the radical polymerization the short-time of radicals associated to the existence of termination reactions hampers the over the polymer structure (Figure 3).

To overcome the limitations of these two approaches, the controlled/living radical polymerization (CLRP) methods made possible the synthesis of polymers with controlled molecular weight, narrow molecular weight distributions, architecture, composition, topology and functionality (Matyjaszewski and Tsarevsky 2009). Among the different CLRP based methods, , the nitroxide-mediated polymerization (NMP), reversible addition fragmentation chain transfer polymerization (RAFT), and atom transfer radical polymerization (ATRP) (Mueller, Jakubowski et al. 2007) are the most broadly used.

ATRP was the chosen method to prepare the several block copolymers used for this work, since this commonly explored CLRP method is simple, efficient, high tolerant to monomer functionality and most of the compounds are available commercially (Rocha, Mendonça et al. 2013). ATRP is a method based in an equilibrium between propagating radicals and dormant species (macroinitiators P_n-X, where X represents a halogen or pseudohalogen) (Cordeiro, Rocha et al. 2013). The dormant species in this equilibrium, that can be polymer chains capable to grow in one or more directions, react with activators which are transition metal complexes in their lower oxidation stage (Mt^m/L, where Mt^m represents the transition metal species in oxidation state *m* and L is a ligand). With that reaction, growing radicals are formed ($P_n^{\bullet}$) intermittently, and deactivators, corresponding to the metal complexes in their higher oxidation state, coordinated with halide ligands X-Mt^{m+1}/L (Figure 4) (Matyjaszewski 2012).

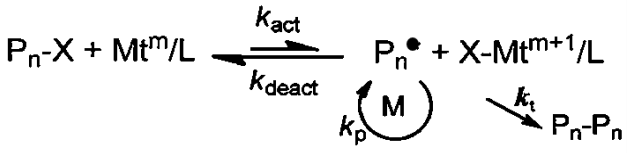

Figure 4 – Equilibrium/propagation expression for ATRP method (Davis and Matyjaszewski 2000).

The dormant species react periodically with the transition metal complexes in their lower oxidation state with a rate constant of activation (k_{act}), and further react with the

deactivators in a reverse reaction (k_{deact}), to re-form the dormant species and the activator (Matyjaszewski 2012). The polymer chains grow between each activation/deactivation cycle, induced by the halide abstraction and subsequent transfer that occurs repeatedly, as mentioned above (Lazzari, Liu et al. 2007).

ATRP is a catalytic process and can be successfully mediated by several redox-active transition metal complexes, such as Ti, Mo; Re, Fe, Ru, Os, Co, Ni, Pd and Cu, where the Cu complexes are most studied catalysts in the ATRP of a wide range of monomers in diverse media (Braunecker and Matyjaszewski 2007). Additionally, the dynamic equilibrium between dormant species and propagating radicals can be easily adjusted by modification of the catalyst's complexing ligand (Braunecker and Matyjaszewski 2007).

The control of molecular weight is accomplished because both initiation and deactivation are fast, allowing the growth of all chains approximately at the same time, while maintaining a low concentration of active species. Termination reactions cannot be fully avoided, however the proportion between the terminated chains and the number of propagating chains is very small ($\leq$ 10%) (Davis and Matyjaszewski 2000). In order to get well defined polymers with narrow polydispersities, the halogen group X must migrate between the growing chain and the transition metal complex in a quickly and selectively way.

ATRP allows preparing polymers containing a terminal radically transferable atoms, usually an halogen, capable to participate in reactions posterior to its polymerisation (re-initiation), or serving as macroinitiators in the synthesis of block copolymers (Matyjaszewski and Tsarevsky 2009). On drawback of this polymerisation technique until recently was the employment of relatively high amount of transition metal complexes (0.1 - 1% in reaction mixture), that had to be removed from the final polymer (Qiu, Charleux et al. 2001; Lazzari, Liu et al. 2007). Recently, the amount of transition metal complex has been remarkably reduced to a few ppm (Matyjaszewski and Tsarevsky 2009). Transversely to all CLRP methods, an appropriate temperature has to be found in such a way, which grants an ideal balance between control over polymerisation (narrow PDIs) and polymerisation rate (conversion) (De Clercq, Laperre et al. 2005).

To evaluate the livingness of the polymers obtained by ATRP, the determination of the molecular weight and polydispersity ($Đ$) are very important. Polymers generally consist in very long chains with different lengths. The polymer chain length is an important characteristic, which influence its properties, and can be expressed quite adequately by the mean of molecular weight. However, since polymers usually are a mixture of different chain

lengths, a uniform molecular weight does not exist, but instead, a molecular weight average (Mulder 1996).

The number-average molecular weight M_n is defined as shown in Figure 5 (a), where n_i is the number of chain of exact molecular weight M_i and ith component has a degree of polymerization i. In this equation, the greater the mass that some polymer's chain, the greater will be the contribution. To reduce the impact of these chains with greater molecular weight, but present in small quantity, was defined the weight-average molecular weight M_w, expressed mathematically as shown in Figure 5 (b). The ratio between M_w and M_n is called the polydispersity index, and frequently abbreviated as $Đ$ Figure 5 (c). For monodisperse polymers, $Đ$ is equal to 1, which means that all chains have the same molecular weight, therefore M_w is equal M_n. For non- monodisperse polymers, the $Đ$ is higher than 1 meaning a broader molecular weight distribution (Teraoka 2002).

In this work, the molecular weight values of the diverse polymers were determined through gel permeation chromatography (GPC).

$$M_{\mathrm{n}} = \sum_i n_i M_i / \sum_i n_i \qquad \text{(a)}$$

$$M_{\mathrm{w}} = \sum_i n_i M_i^{\,2} / \sum_i n_i M_i \qquad \text{(b)}$$

$$\mathrm{PDI} = \frac{M_{\mathrm{w}}}{M_{\mathrm{n}}} = \sum_i n_i \sum_i n_i M_i^{\,2} \Big/ \left(\sum_i n_i M_i \right)^2 \qquad \text{(c)}$$

Figure 5 – Molecular weight determination of polymers: (a) number-average molecular weight; (b) weight-average molecular weight; (c) polydispersity index (Teraoka 2002).

2.4. Taylor-made structure

Polymers developed to act as protective agents or steric stabilizers, must be strongly anchored to the particle surface. This connection should be made at least by one point, or even better, through several points. When a single point attachment is involved, the remaining polymer chain will be a free-swinging “tail” that is projected into the solution (Figure 6 (a)), providing a protective layer, generally called by steric stabilization (Myers 1991). If two or more points are involved in the connection between polymer and the surface, the result will be the formation of various “trains” and “loops”, since not all sites of polymeric chain possess points are capable to link at surface, and possible formation of “tails” too (Figure 6 (b))

(Myers 1991). “Trains” are the segments connected at the surface, while the segments that are bounded by "trains" in both sides, and which are not connected to the surface, are called by “loops” (Farrokhpay 2009). Both “tails” as “loops”, consist in groups that have no interactions with the surface.

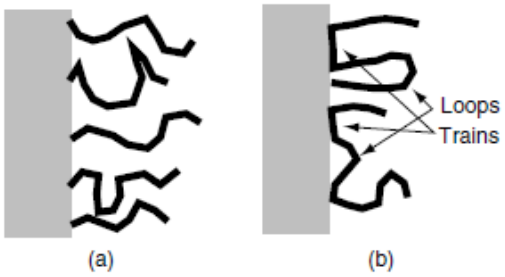

Figure 6 – Two different ways of a polymer adsorb in a surface. Adsorbed at one end of the chain producing “tails” (a), or adsorbed at several points producing “loops” and “tails” as in (b) (Myers 1991).

Variations in length of the “trains”, “loops” and “tails” control the conformation of adsorbed polymer, and therefore layer thickness. In fact, for a given polymer chain length, a system composed only by “tails”, in which these “tails” extend into the solution, the protective layer will be greater than a comparable system of “loops” (Myers 1991).

In fact, it could be envisaged that a single-point attachment would provide a better protection due to the greater protective layer. However in a “loops” conformation, when an interpenetration begins, there will be twice or more units affected by the volume restriction effect, leading to a stronger entropic effect. It is not possible to affirm that one configuration is better than another, but in the most of the cases, both configurations will be present (Myers 1991). According to Farrokhpay, an effective stabilization requires a high coverage, effective anchoring, extended “tails” (and possible “loops”) and a good solvent for the segments to be in “tails” and/or “loops” (Farrokhpay 2009).

In the case of anionic polymers, the adsorption is strongly dependent on the degree of functional group dissociation, pH of solution and ionic strength values. At pH values where there is not dissociation, the polymer behaves as a non-ionic polymer, with relatively short “loops” and long “tails” (Farrokhpay 2009). At low ionic strength solutions, ionic polymers possess an extended conformation and adsorb in thin layers of flat conformations, while at high ionic strength, the electrostatic repulsion is reduced and the adsorbed layer thickness increases due to the occurrence of “loops” and “tails” (Farrokhpay 2009). This type of

conformations originated by the connection of the studied copolymers with the surface of the TiO_2 particles are expected to provide a barrier against the particles flocculation.

2.5. Self-Assembly of copolymers

Amphiphilic block copolymers, which are composed by blocks/segments with different solubilities, tend to self-assemble and form micellar structures when they are diluted in a medium that has selective solubility for one of these segments. The micellar structure consists of a core formed by the aggregated insoluble blocks of the copolymer, surrounded by a spherical corona shell formed by the soluble blocks (Yang, Su et al. 2007). The presence of micelles leads to significant differences in structural and flow characteristics of the polymer in solution. (Hamley 2004).

Like in surfactants case, block copolymers only form micelles if they are above a certain concentration, which is known as critical micelle concentration (CMC) (Hamley 2004). Therefore, to ensure micelles formation it is necessary to have a quantity of block copolymer in solution with a final concentration higher than the CMC. Usually a few milligrams per liter are sufficient to have micelles formation, as the example of some surfactants that possess values in a range of 0.6 g/L to 20 g/L (Myers 1991). It is reported some CMC values for block copolymers, wherein at least one of the blocks is P4VP and molecular weights that vary from 7000 to 20500 g/mol, being that CMC values have a range of 5 to 87 mg/L (Creutz and Jérôme 1999). There are also some CMC values reported for copolymers where at least one of the blocks is DMAEMA and with molecular weights between 5300 and 17000 g/mol, in which CMC varies from 15 to 340 mg/L (Creutz and Jérôme 2000). Since the minimum copolymer concentration used in the tests (1 mg/mL) is well above the mentioned values for 4VP and DMAEMA copolymers) the formation of micelles is expected. For the other copolymers used, it is believed that the CMC has also been passed, since generally a few milligrams per liter are sufficient to form micelles. The formation micelles structures were confirmed by DLS results, as will be seen later.

The aim of these structures formation in an aqueous medium is to bind and stabilize TiO_2 particles in the micelle core, composed by the hydrophobic segment, since that TiO_2 is insoluble in aqueous medium.

2.6. Particles stabilization

The stabilization of pigment particles with polymeric dispersants is generally due to two mechanisms, charge or electrostatic stabilization and steric stabilization. Both mechanisms can be present, and in this case, the stabilization is called electrosteric. A schematic diagram of these three mechanisms to stabilize particles in suspension is shown in Figure 7 (Farrokhpay 2009).

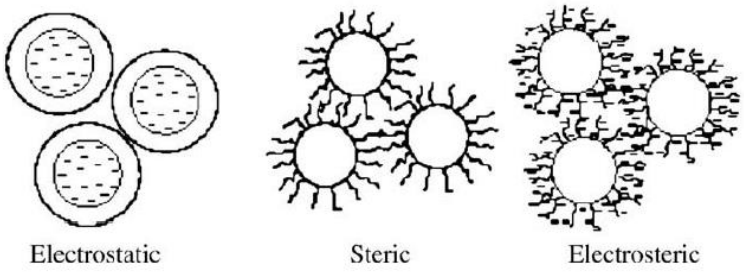

Figure 7 – Stabilization mechanisms in particle suspensions (Farrokhpay 2009).

Electrostatic stabilization in an aqueous system involves ionic polymers adsorbed onto pigment surface, copolymer that is charged accordingly and surrounded by a diffuse electrical layer of the opposite sign (Creutz, Jerome et al. 1998; Farrokhpay 2009). When two particles get closer, an overlap of the diffuse layer of both particles starts resulting in electrostatic repulsion, which increases with the interparticle distance reduction. The main drawback of this stabilization mechanism, is the high sensitivity to the aqueous phase ionic strength, which can shield out the chemisorbed charges and lead flocculation (Creutz, Jerome et al. 1998). Beyond that, the stabilizing charge from the ionic polymer can be readily reduced by the presence of external influences, like surface or ionic solution impurities, or with addition of other pigments with different surface charge properties (Farrokhpay 2009).

The steric stabilization, on the other hand, is due to 2 factors: a volume restriction component and a mixing or osmotic component, involving compression of the adsorbed layer, that do not allow the sufficient particles approach to flocculate. Ionic polymeric dispersants can provide both electrostatic and steric stabilization, while non-ionic polymeric dispersants can only stabilize the particles via a steric force (Farrokhpay 2009). Ionic dispersants can be used in small amounts, but they are sensitive to the presence of multivalent ions, pH and ionic

strength, while nonionic dispersants are not sensitive to the pH, but must be used in higher concentrations (Farrokhpay 2009).

A diblock copolymer consisting in a hydrophobic block (anchoring block) associated with a polyelectrolyte block, has the advantage of comprising, beyond the steric barrier provided by hydrophobic group, the additional capability of repelling the particles from each other by electrostatic repulsion. Particles stabilized by this kind of mechanism can tolerate a higher ionic strength, since the steric stabilization can compensate a decreased thickness of the diffuse electrical layer (Creutz, Jerome et al. 1998).

When very high molecular polymers with more than one potential attachment point to the particle surface are used as stabilizers, the possibility of various points of attachment to connect different particles exist, rather than connect to the same particle. This happens often when there is a large excess of particles relative to the concentration of polymer. But, when this attachment of the same polymer chain to two or more particles takes place, essentially ties the particles together and brings them closer, in effect sensitizing the particles to flocculation, a process called bridging flocculation, which is illustrated in Figure 8 (b) (Myers 1991).

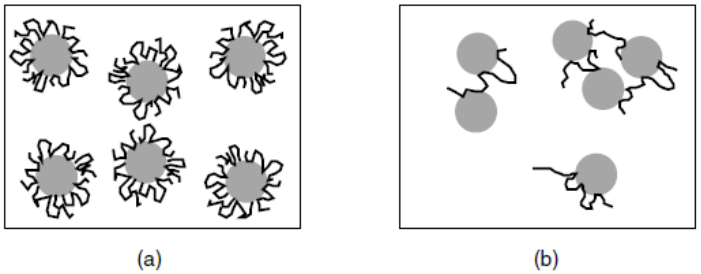

Figure 8 – In sterically stabilized systems, a given adsorbed polymer molecule will be associated with one particle (a). In systems containing a low polymer concentration and/or very high molecular weight polymer, molecules can become adsorbed to two or more particles leading to ‘‘bridging’’ flocculation (b).

In case of a poorly adsorbed polymer into particle surface, or even when the polymer cannot be connected to particles, another phenomenon may occur, and it is termed depletion flocculation. In depletion flocculation, when two particles approach and the polymer chain is weakly adsorbed, or simply are located between the particles, become squeezed out of the area of closest approach, leaving the surfaces that are attracted, for example by Van der Waals attractive forces, unprotected. When the particles approach, the polymer is forced out of the area between them, resulting in particles flocculation, how can be seen in Figure 9 (Myers 1991).

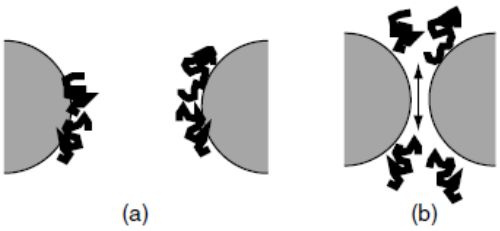

Figure 9 – In a sterically stabilized system containing low-molecular-weight or weakly adsorbed polymer (*a*), as two particles approach, the loosely bound polymer may desorb, leaving ‘‘bare’’ spots on the approaching surfaces, leading to an enhanced flocculation tendency (*b*) (Myers 1991).

Hence, for the stabilization of TiO_2 particles, it is necessary to have polymers in which molecular weight should not be very high, and thus, not having many attachment points to prevent bridging flocculation, and should be strongly connected to particles surface in order to avoid depletion flocculation.

2.7. Commercial dispersants

Industrially, the most widely dispersants used and that are capable of dispersing titania pigment particles in water-based paint formulation are based on polyacrylic acid and/or polyacrylamide, providing a smooth and glossy surface (Farrokhpay, Morris et al. 2005; Farrokhpay, Morris et al. 2010). As demonstrated by Farrokhpay et al, the most likely mechanism of TiO_2 stabilization provided from these polymers is through electrostatic interactions (Farrokhpay, Morris et al. 2010). The performance obtained using these materials in commercial paints are still far from desired in terms of the TiO_2 dispersion.

Some studies were carried out in order to find other polymers capable to stabilize TiO_2 particles, and to be an alternative to the copolymers industrially used. Serge Creutz and Robert Jérôme (1999) reported the use of diblock copolymers containing a polyelectrolyte block of sodium methacrylate (MANa), and a hydrophobic block of 4-vinylpyridine (4VP) and 2-vinylpyridine (2VP), which act as anchoring block to titania surface. Poly4VP and poly2VP blocks have proved to be strongly anchoring blocks toward TiO_2, and due also to the presence of a polyelectrolyte block, the particles possess a electrosteric barrier against coalescence, and in their study, depletion flocculation did not occur (Creutz and Jérôme 1999).

In 2000, also Serge Creutz and Robert Jérôme, reported the dispersing titanium dioxide efficiency in a high solid content dispersion, using for this case a block copolymer of 2-(dimethylamino)ethyl methacrylate (DMAEMA) and MANa. In this case, PDMAEMA block acts as anchoring block, which can interact with the alumina present in TiO_2 particles surface through hydrogen bonding and Lewis acid-base interactions, as well in the P4VP case. As above, MANa block provides the electrostatic interaction while PDMAEMA provides a steric stabilization (Creutz and Jérôme 2000).

In 2013, F. Karakas and M.S. Çelik, reported that sodium polyacrylate (NaPAA), which is also generally used as a dispersant in paint formulations on the stability of alumina-coated TiO_2 suspensions, provides an electrostatic repulsion and stable dispersion when used in proper concentrations. The required concentrations to achieve a stable dispersion will depend mainly of the pH values and the solid loadings of TiO_2 (Karakas and Celik 2013).

The block copolymers used in this thesis for TiO_2 stabilization will consist in two blocks, one hydrophobic that will anchor to the surface of TiO_2 particles providing a steric stabilization, and the other block will be hydrophilic, which will provide not only a steric and/or electrosteric stabilization as helping dispersing the particles into aqueous medium. Two of the hydrophobic groups will be of P4VP and PDMAEMA, since both segments have good anchoring properties to the alumina surface of titania pigments, and one of the hydrophilic groups will be formed by PAA, since it can offer both steric and electrostatic stabilization.

2.8. Titanium Dioxide

2.8.1. General Remarks

Titania, or titanium dioxide (TiO_2), is present in the nature in three crystallographic phases: anatase, rutile and brookite, being the anatase and the rutile phase the most important ones, which are produced industrially in large amounts to be used in several diverse areas (Buxbaum and Pfaff 2005; Wei, Zhu et al. 2013).

TiO_2 can be produced from natural products as ilmenite, leucoxene ores and rutile, and from some synthetic materials such as titanium slag and synthetic rutile. Its manufacture can be achieved by using either the sulphate or the chloride process (Buxbaum and Pfaff 2005;

Farrokhpay 2009). The chloride process is a more recent than the sulphate process, producing much less and safer waste material, although it is more expensive at small scale operations (Farrokhpay 2009).

The sulfate process starts with dissolution of the titanium-containing raw material in concentrated sulfuric acid at 150 – 220 ºC, originating a "black liquor". Relatively pure TiO_2 dehydrate is then precipitate by hydrolysis of this sulfate solution. Impurities are mostly removed in further purification stages. The resultant TiO_2 is then calcined, ground and surface treated, which consists in a coating stage with inorganic compounds (Buxbaum and Pfaff 2005; Farrokhpay 2009).

In the chloride process, the titanium raw materials are chlorinated to form titanium tetrachloride at 700 – 1200 ºC. After impurities removal and further fractional distillation, the pure titanium tetrachloride is oxidized at temperatures of 900 – 1400 ºC to form TiO_2. This raw pigment is also ground and coated with inorganic compounds (Buxbaum and Pfaff 2005; Farrokhpay 2009).

2.8.2. Applications of TiO_2

TiO_2 is worldwide used, being the most important pigment in terms of quantity and value, with about 4.2×10^6 t being produced in 2003, its consumption has been growing over the years. The leading market segments on the TiO_2 consumption in the 2003 year were coatings (57%), plastics (22%) and paper (12%)(Buxbaum and Pfaff 2005).

Due to its versatility, TiO_2 is a material widely used in a number of technologically important application, like catalyst, white pigment for paints or cosmetics, electrodes in lithium batteries, etc. (Wei, Zhu et al. 2013).

In nanometric dimension, titania particles can be used for water treatment, as antibacterial and air purification due to their effective photocatalytic activity (Othman, Abdul Rashid et al. 2012).

2.8.3. Surface/Properties of TiO_2

TiO_2 is highly stable and is regarded as completely nontoxic, and among the three main crystal phases of TiO_2 mentioned above, rutile is the thermodynamically most stable one, whereas anatase and brookite are metastable phases that are easily transformed in rutile by thermal treatment (Buxbaum and Pfaff 2005; Wei, Zhu et al. 2013).

Both anatase and rutile crystal forms are used as prime pigments in paint and coating industries. However, paints with a greater content of rutile are preferred, since paints with rutile are more stable on outdoor exposure than those containing anatase, and have a higher hiding power than anatase. In fact, the refractive index (RI), which measures the ability of a substance to bend light (Lambourne and Strivens 1999), of rutile form is the highest of all known white pigments, with a RI of 2.76, against the 2.55 of anatase, providing highest refractive light scattering and therefore the highest opacity (Farrokhpay 2009).

Another advantage of using titania pigment over other inorganic pigments, concerns to the ability of prepare particles with a relatively narrow particle size distribution. These control on the particles size, is an important parameter once the optimum crystal and particle size allows to obtain the maximum scattering of visible light (Farrokhpay 2009). For maximum opacity, the desired particle size should be approximately half the dominant wavelength (Lambourne and Strivens 1999). Thus, once the range of visible light wavelengths is 400 – 700 nm, the theoretical value for the particles size should not be less than 200 – 350 nm. In practice, since human eye is most sensitive to yellow - green light with a wavelength of about 560 nm, titania particle sizes is usually 200 – 300 nm. (Farrokhpay 2009).

In the end of TiO_2 manufacturing process, its surface is coated with inorganic oxides such as alumina, silica or zirconium followed by alumina, in order to optimize the pigment application performance including the reduction of photo-catalytic activity and the improvement of dispersion and gloss properties. The alumina present in titania surface is thought to provide better particle dispersion through decreasing the effect of Van der Waals attractive forces. Furthermore, alumina-doped titania pigments have only a few, if any, Ti – OH surface sites, and because of aluminum surface treatment, polymeric dispersants have been shown to have strong adsorption on the rutile crystal form (Farrokhpay 2009).

3. Experimental

3.1. Materials

The titania pigments sample used throughout this study was a typical commercial pigment for the paint industry with the trade name KEMIRA, kindly granted by Resiquímica. This sample is mostly composed by rutile crystal form. The involved surface treatment, was Al_2O_3, SiO_2 and other organic compounds and a minimum TiO_2 content of about 93%. The particles have a mean crystal size about 220 nm, refractive index of 2.7 and pH of 7.6 - 8.6. The polymeric dispersant of commercial name Additol VXW 6200, kindly granted by Resiquímica, was used as reference in this work to evaluate the performance of the new block copolymers as dispersants.

Both poly(ethylene glycol) methyl ether (mPEG) ($mPEG_{113}$: Mw=5000 Da, and $mPEG_{45}$: Mw=2500 Da; Sigma-Aldrich) were dried by azeotropic distillation from toluene. 2-chloropropionyl chloride (CPC) (97%; Sigma-Aldrich), 2-Bromoisobutyryl bromide (BBiB) (98%; Sigma-Aldrich), $CuCl_2$ (+99% extra pure, anhydrous; Acros) were used as supplied. Cu (0) wire (99%; Acros) was activated with nitric acid, washed with acetone and dried before use. Isopropanol (IPA) (99.97%; Fisher Chemical), ethanol (96%; Panreac), diethyl ether (>99.8%; Sigma-Aldrich), deuterated dimethyl sulfoxide (DMSO) (+99%; Sigma-Aldrich), Deuterium oxide (D_2O) (+99%; Sigma-Aldrich), Trifluoroacetic acid (TFA) (99%; Sigma-Aldrich), methanol (MeOH) (>99.85%; Aldrich), chloroform (99.99%; Fisher Chemical), dimethylformamide (DMF) (+99.8%; Sigma-Aldrich), deuterated chloroform ($CDCl_3$) (+1% tetramethylsilane (TMS); Euriso-top), sodium hydroxide (pellets QP; Panreac) and hydrochloric acid solution (HCl) (37%; Aldrich) were used as received. Milli-Q water (Milli-Q®, Millipore) was obtained by reverse osmosis. 4-vinylpyridine (4VP) (96%; Fluka) was dried and distilled under reduced pressure, prior to use. Triethylamine (TEA) (96%; Sigma-Aldrich) was distilled and stored over molecular sieves, and dichloromethane (DCM) (+99.6%; Fisher Scientific) was dried and distilled over calcium hydride dried, and stored over molecular sieves, prior to use. 4-Dimethylaminopyridine (DMAP) (+99%; Sigma-Aldrich) was recrystallized from toluene. Tris(2-dimethylaminoethyl)amine (Me6TREN) was synthesized according to procedures described in the literature (Ciampolini and Nardi 1966). For Gel Permeation Chromatography (GPC), poly(methyl methacrylate) (PMMA) standards (Polymer Laboratories) (Acros, 99%, ~70 mesh) and high performance liquid chromatrography (HPLC) DMF (HPLC grade; Panreac) were used as received. Toluene,

acetone, and ethanol were purchased from Ghataran Shimi T. Co. 2-(dimethylamino)ethyl methacrylate (DMAEMA) (Aldrich, 98%) was passed over a sand/alumina column before use in order to remove radical inhibitors. Copper (I) bromide (CuBr) (+98%; Fluka), copper (II) bromide ($CuBr_2$) (+99% extra pure, anhydrous; Acros), tetrahydrofuran (THF) (Fisher Chemical), N,N,N',N'',N''-pentamethyldiethylenetriamine (PMDETA) (99%; Aldrich), iron powder (Fe(0)) (98%; Aldrich) and purified water (Milli-Q®, Millipore, resistivity >18 MU cm) was obtained by reverse osmosis.

3.2. Characterization

3.2.1. Gel Permeation Chromatography (GPC)

Gel permeation chromatography (GPC) was carried out using high performance size-exclusion chromatography (HPSEC), with refractive index (RI) (Knauer K-2301) detection. The column set consisted of a PL 10-µL guard column (50 x 7.5 mm^2), followed by two MIXED-B PL columns (300 x 7.5mm^2, 10µL). The HPLC pump was set with a flow rate of 1 mL/min and the analyses were carried out at 60 ºC using an Elder CH-150 heater. The eluent was DMF, containing 0.3% of LiBr. Before injection (100µL), the samples were filtered through a polytetrafluoroethylene (PTFE) membrane with 0.2µm pore size. The system was calibrated against PMMA standards.

The molecular weights and polydispersity index (*Đ*) of macroinitiators and diblock copolymers synthetized and used across the work, were characterized by GPC using conventional calibration, where 4 mg of each sample, after the respective purification step, was weighted and dissolved in DMF to GPC analysis.

3.2.2. Nuclear Magnetic Resonance (^{1}H-NMR Spectra)

400 MHz ^{1}H NMR spectra of each reaction mixture samples, recovered products, before hydrolysis, and macroinitiators were recorded on a Bruker Avance III 400MHz spectrometer, with a 5-mm TIX triple resonance detection probe, in $CDCl_3$ with tetramethylsilane (TMS) as an internal standard. The mPEG-*b*-PAA and PAA-*b*-PDMAEMA copolymers, after hydrolysis of PtBA segment, were analyzed in deuterated DMSO with TMS as an internal

standard. In case of the PAA-*b*-P4VP copolymer, was analyzed both in D_2O, with pH = 2 by addition of 1M HCl, as DMSO, also with TMS as an internal standard. The conversion of macroinitiators and block copolymers compositions were determined by integration of the monomer and polymer peaks using the MestRenova software, version 6.0.2-5475.

The ^{1}H-NMR analysis allowed to determine the conversions achieved in each reaction and the number of repeating units (chain length). For the conversion calculations, circa of 4 drops from the reaction solution were mixed with about between 600 and 700µL of $CDCl_3$. In the case of the chain length, the samples used were from the purified polymer, where 10mg of each polymer were weighed, mixed with about 600-700 µL. For mPEG-*b*-PAA and PAA-*b*-PDMAEMA around 5mg of purified copolymers were dissolved in 300-400 µL of deuterated DMSO and analyzed by ^{1}H-NMR, in order to confirm the PtBA segment hydrolysis. In the case of PAA-*b*-P4VP, since the ^{1}H-NMR with DMSO did not show well defined peaks corresponding to P4VP group, a second ^{1}H-NMR with D_2O and acidic pH, as reported by (Bo and Zhao 2006), was performed to ensure that P4VP groups did not suffer any change during the hydrolysis reaction. 5mg of pure PAA-*b*-P4VP were weighted, and dissolved in around 300-400 µL of DMSO, while another 5mg were weighted and dissolved in about 300-400 µL of D_2O and pH adjusted to acidic, in order to identify the P4VP peaks.

3.3. Synthesis of macro initiators

3.3.1. Synthesis of mPEG

The $mPEG_{113}$-Cl was prepared through an adaptation of a reported method (Zhang, Shi et al. 2005). DMAP (0.916g, 7.5mmol), DCM (20 mL) and TEA (0.7mL, 5mmol) were placed into a round-bottom flask. A solution of CPC (1.21mL, 12.5mmol) in DCM (20 mL) was then added dropwise and a yellow dispersion was formed. After, $mPEG_{113}$ (10.0g, 5.0mmol) and DCM (30mL) were added, under a N_2 atmosphere in an ice bath (0ºC). After the CPC solution addition, the temperature was kept at 25ºC and the reaction continued under magnetic stirring for 18 h. The obtained dispersion was then filtered, concentrated by solvent evaporation and the product recovered by precipitation in cold diethyl ether. The crude product was purified by recrystallization overnight in absolute ethanol. After being filtered and washed with cold diethyl ether, the macroinitiator was collected and dried for 48 h, under vacuum, at 40ºC. The same procedure was used for the preparation of $mPEG_{45}$-Cl. A similar

procedure was used for the preparation of $mPEG_{113}$-Br and $mPEG_{45}$-Br, but required the use of 2-Bromoisobutyryl bromide (BBiB) instead of CPC.

3.3.2. Synthesis of PtBA

PtBA macroinitiator was prepared adapting a reported method by (Davis and Matyjaszewski 2000). CuBr (39.1mg, 2.73×10^{-4}mol) and $CuBr_2$ (3.0mg, 1.4×10^{-5}mol) were added to a dry round-bottom flask. The flask was sealed with a rubber septum, degassed and back-filled with nitrogen three times, and left under nitrogen. Deoxygenated acetone (1mL) was added, after which tBA (4.0mL, 2.7×10^{-2}mol) was added, both via syringes that had been purged with nitrogen. PMDETA (60μL, 2.9×10^{-4} mol) was added, and the solution was stirred until the Cu complex had formed. This is easily visualized through a change of the solution from cloudy and colorless to clear and light green. After complex formation, methyl 2-bromopropionate (MBP) (61μL, 5.5×10^{-4}mol) was added to the flask, an initial sample was removed, and the flask was placed in an oil bath thermostated at 60°C. After the desired reaction time, the reaction was stopped by immersing the flask into liquid N_2 and a sample was taken to determine the monomer conversion by ^{1}H NMR spectroscopy. Then, the macroinitiator was dissolved in additional acetone and filtered through a column of alumina to remove the copper catalyst from the polymer. The acetone was removed by evaporation, and the polymer was then precipitated into a 10-fold excess of a 50:50 v:v water:MeOH solution. The final product obtained was filtered and then dried, under vacuum for 24h.

3.4. Synthesis of the block copolymers

3.4.1. Synthesis of mPEG-*b*-PDMAEMA

mPEG-*b*-PDMAEMA block copolymers were synthetized according to (Rocha, Rodrigues et al. 2014), using Fe(0) and [$CuBr_2$]/[PMDETA]=0.1/1.1 catalytic system in IPA/H2O (9:1) at 50ºC in a N_2 atmosphere. In a typical procedure, $mPEG_{113}$-Br (1.648g, 0.33mmol), IPA (4.5mL) and Fe(0) (18.4mg, 033mmol) were placed in a Schlenk reactor. In a vial, PMDETA (62.9mg, 0.36mmol) was added to DMAEMA (5mL, 30mmol), and in another vial $CuBr_2$ (62.34mg, 0.03mmol) was dissolved in H_2O (0.5mL). Then both solutions were

added to the Schlenk flask and immediately frozen in liquid nitrogen, the system was deoxygenated with four freeze-vacuum-thaw cycles and purged with nitrogen. The Schlenk reactor was then placed in a pre-heated oil bath at 50ºC and left reacting under magnetic stirring. After the desired reaction time, the reaction was stopped by immersing the flask into liquid N_2 and a sample was taken to determine the monomer conversion by ^{1}H NMR spectroscopy. Then, the block copolymer was precipitated in hexane, dissolved in THF and passed through an alumina column to remove the copper and iron catalysts. The solution was concentrated by rotary evaporation and the product recovered by precipitation in hexane, followed by centrifugation. The crude product was dried under vacuum, at 40ºC for 48h.

3.4.2. Synthesis of mPEG-*b*-P$_4$VP

mPEG$_{113}$-*b*-P4VP block copolymers were prepared according to (Rocha, Mendes et al. 2014), using a catalytic system of Cu(0) and [$CuCl_2$]/[Me_6TREN]=1/1. In a typical procedure, a mixture of mPEG$_{113}$-Cl (0.472g, 0.09mmol), $CuCl_2$ (12.47mg, 0.09mmol), Me_6TREN (21.36mg, 0.09mmol) and IPA (3.11 mL) was placed in a Schlenk reactor and immediately frozen in liquid nitrogen. Activated Cu(0) wire was placed in the reactor and the system was deoxygenated with four freeze-vacuum-thaw cycles and purged with nitrogen. 4VP (3.0mL, 28mmol) was then added to a Schlenk reaction vessel under a nitrogen atmosphere and the reaction mixture was immediately frozen in liquid nitrogen and deoxygenated by conducting three freeze-vacuum-thaw cycles and purged with nitrogen. The Schlenk reactor was placed in a pre-heated oil bath at 50ºC and left reacting under magnetic stirring. After the desired reaction time, the reaction was terminated by immersing the flask into liquid N_2 and a sample was taken to determine the monomer conversion by ^{1}H NMR spectroscopy. Then, the block copolymer was precipitated in cold diethyl ether and the solid dissolved in chloroform and passed through an alumina column to remove the copper catalyst. The solution was concentrated by rotary evaporation and the product recovered by precipitation in cold diethyl ether, followed by filtration. Further catalysts removal was achieved by re-dissolving the product in methanol and dialysis for 12h (molecular weight cut-off (MWCO) = 3500Da). Finally, the crude product was obtained by precipitation in cold diethyl ether, filtered and then dried, under vacuum, at 40ºC for 48h. A similar procedure was used for the preparation of mPEG$_{45}$-*b*-P4VP block copolymers, adjusting the mass of mPEG$_{45}$.

3.4.3. Synthesis of PAA-*b*-P$_4$VP

PtBA-*b*-P4VP block copolymer, and sequential PtBA block hydrolysis, was prepared through adaptation of the reported method by (Wehrung, Li et al. 2013). In a typical procedure, $CuCl_2$ (16mg, 0.16mmol), P*t*BA-Br (1.0g, 0.13mmol), Me_6-TREN (36.8mg, 0.16mmol), DMF (4.0mL) and activated Cu(0) wire, were added successively into a Schlenk reactor, and the system was deoxygenated with four freeze-vacuum-thaw cycles and purged with nitrogen. 4VP (1.6g, 15.0mmol) was added via a gastight syringe and the mixture was degassed one more time, with three freeze-evacuate-thaw cycles followed by immersing the flask into an oil bath preset at 80ºC. After the desired reaction time, the reaction was terminated by immersing the flask into liquid N_2 and a sample was taken to determine the monomer conversion by ^{1}H NMR spectroscopy. PtBA-*b*-P4VP was then diluted with THF and passed through a column of neutral alumina to remove the metal salt, and the solution was concentrated by rotary evaporation. The formed P*t*BA-*b*-P4VP was further purified by precipitation in a water/methanol mixture (1/3 v/v) three times, filter and dried under vacuum.

The hydrolysis of PtBA segment was accomplished by using the following procedure: typically, PtBA-*b*-P4VP (1g) was firstly dissolved into dried DCM (8mL) in a round-bottom flask. After complete dissolution, TFA (1.5mL) was added into polymer solution, drop-by-drop via a gastight syringe and under N_2 atmosphere, in an ice bath (0ºC). After the TFA addition, temperature was kept at 25ºC and the reaction was left overnight under magnetic stirring. The resultant mixture was dissolved in DCM, precipitated in diethyl ether three times, and dried under vacuum at room temperature.

3.4.4. Synthesis of PAA-*b*-PDMAEMA

PtBA-b-PDMAEMA block copolymer was prepared through adaptation of reported method by (Zhang, Ai et al. 2011), followed by hydrolysis of PtBA block segments using an adaptation of a reported method (Wehrung, Li et al. 2013). In a typical procedure P*t*BA-Br (0.5 g, 0.12mmol), PMDETA (24.8µL, 0.12mmol), IPA (1.8mL), Cu(0) powder (7.5mg, 0.12mmol) and $CuBr_2$ (2.65mg, 0.01mmol) dissolved in DMF (0.2mL) were added successively into a Schlenk reactor, and the system was deoxygenated with four freeze-vacuum-thaw cycles and purged with nitrogen. DMAEMA (1.9g, 12mmol) was added via a gastight syringe

and the mixture was degassed with three freeze-evacuate-thaw cycles followed by immersing the flask into an oil bath preset at 50ºC. After the desired reaction time, the reaction was terminated by immersing the flask into liquid N_2 and a sample was taken to determine the monomer conversion by ^{1}H NMR spectroscopy. PtBA-*b*-PDMAEMA was then dissolved with $CHCl_3$ and passed through a column of neutral alumina to remove the metal salt, and the solution was concentrated by rotary evaporation. The formed P*t*BA-*b*-PDMAEMA was further purified by precipitation in diethyl ether, filter and dried under vacuum.

The PtBA block was hydrolyzed by adaptation of the previously cited report (Wehrung, Li et al. 2013). In a typical procedure, PtBA-*b*-PDMAEMA (1g) was firstly dissolved into dried DCM (8mL) in a round-bottom flask, in order to dissolve the copolymer. After complete dissolution, TFA (1.5mL) was added into polymer solution, drop-by-drop via a gastight syringe and under a N_2 atmosphere, in an ice bath (0ºC). After the TFA addition, temperature was raised to 25ºC and the reaction was left overnight under magnetic stirring. The resultant mixture was then dissolved in MeOH, precipitated in diethyl ether three times and dried under vacuum at room temperature.

3.4.5. Synthesis of mPEG-*b*-PAA

The mPEG-*b*-PtBA was prepared through an adaptation of a reported method (Yuan, Chen et al. 2012), and posterior hydrolysis of PtBA segment into PAA was accomplished by the adaption of a typical procedure described in (Martinez-Castro, Zhou et al. 2010). In a typical procedure of mPEG-*b*-PtBA polymerization, PEG-Cl (1.0g, 0.2mmol Cl group) and $CuCl_2$ (28.7mg, 0.2mmol) were placed in a Schlenk reactor and immediately frozen in liquid nitrogen. Activated Cu(0) wire was placed in the reactor and the system was deoxygenated with four freeze-vacuum-thaw cycles and purged with nitrogen. tBA (2.3mL, 16mmol), dry acetone (10mL), and PMDETA (50µL, 0.24mmol) were introduced via a gastight syringe. The mixture was degassed with three freeze-evacuate-thaw cycles followed by immersing the flask into an oil bath preset at 60ºC. After the desired reaction time, the reaction was terminated by immersing the flask into liquid N_2 and a sample was taken to determine the monomer conversion by ^{1}H NMR spectroscopy. The reaction mixture was diluted with THF and passed through a short neutral alumina column to remove the residual copper catalyst. The filtrate was concentrated by rotary evaporation and precipitated into cold petroleum ether twice. The final product was obtained after drying in vacuum at 40ºC overnight.

To hydrolyze the PtBA block, mPEG-*b*-PtBA (0.98g) and dried DCM (20mL) were placed into a round-bottom flask, in order to dissolve the copolymer. After complete dissolution, trifluoroacetic acid (TFA) (3mL) was added dropwise, via a gastight syringe and under a N_2 atmosphere, in an ice bath (0ºC). After the TFA addition, temperature was raised to 25ºC and the reaction was left overnight under magnetic stirring. The resultant mixture was added into 400mL of diethyl ether in order to precipitate the product, mPEG-*b*-PAA. The precipitate was then re-dissolved into 10mL of DCM and added into diethyl ether again. This procedure was repeated before the final precipitate was dried under vacuum at room temperature.

3.5. Stability and dispersion evaluation

3.5.1. Dynamic light scattering (DLS) and Zeta potential measurements

Dynamic light scattering (DLS) measurements were performed on a Malvern Instruments Zetasizer Nano-ZS (Malvern Instruments Ltd., UK). The particle size distribution (in intensity), average hydrodynamic particle size average (z-average) and polydispersity index (PDI) were determined with Zetasizer 6.20 software. Measurements were made at 25ºC and at a backward scattering angle of 173º. Zeta-potential measurements were performed using the same equipment, to laser Doppler electrophoresis and determined using a Smoluchovski model.

The self-assembly of the block copolymers in the presence and absence of TiO_2 particles was carried out using a solvent evaporation method, as described in Rocha (Rocha, Rodrigues et al. 2014). In this procedure, a 50 mL solution of Milli-Q water with 0.1 mg/mL of TiO_2 particles was prepared, using ultrasonication during 2 min and 90% of amplitude to disperse the particles in the aqueous medium. As mentioned by Othman et al. (Othman, Abdul Rashid et al. 2012), ultrasonication has been proven to be suitable tool to eliminate agglomeration in aqueous suspensions. An amplitude of 90% was chosen to disperse and homogenize the Milli-Q water/TiO_2 mixture, since a higher amplification creates a more intense and efficient disruption. After that, 2 mL of a 50 mg/mL block copolymer solution in THF (for mPEG-*b*-PDMAEMA), MeOH (for mPEG-*b*-P4VP and PAA-*b*-P4VP) or acetone (for mPEG-*b*-PAA and PAA-*b*-PDMAEMA) was added dropwise to the previous dispersion. Each copolymer solution was added under vigorous mechanical stirring and then left stirring

for 24h to evaporate the organic solvent. The pH of each aqueous suspension was adjusted to a near value of 9.5, since it is the range that industry uses to disperse titania pigment (Farrokhpay, Morris et al. 2005).

For DLS measurements, about 1.5 mL of each sample was removed from the suspensions and placed in the plastic cuvette used in the measurements, while for zeta (ς) potential a sample was taken from the top of the suspension, inserted in the capillary cell, and analyzed. The measurements were carried out during 2 weeks. Three measurements of the each sample was performed for both DLS and for ς potential.

3.5.2. Rheological measurements

The viscosity of dispersions were determined at 25ºC, using a Reologica AB ViscoTech with a bob cup geometry (CC25). The test was carried out by continuous stirring from 0 to approximately 1500s^{-1} shear rate, recording 30 measurements through 450s. The viscosity of each sample was measured through the average of the values recorded at the steady state, in this region the viscosity is independent of the shear rate (Newtonian regime) (Cosgrove 2010). For these tests, the samples procedure was similar to that described for the DLS and ς potential tests, changing only the TiO_2 and copolymer concentrations. The concentrations used were 2.80 mg/mL of copolymer and 200 mg/mL of TiO_2, taking as model the proportion 0.28:20 (in weight) of copolymer and TiO_2 respectively, used in a typical paint formulation, which was provided by Resiquímica. A similar formulation can be found in Appendix VI, where dispersing agent (Dispersex GA 40, industrial name) has a solid content of about 40% (BASF, 2014).

It is important to mention that since different proportions of TiO_2 particles and copolymer were used in DLS and ς potential, and for the rheological measurements, the results cannot be directly comparable. For DLS and ς potential, the proportion used was 0.1:1 (TiO_2:copolymer), and for rheology was 20:0.28, since is the ratio used in a typical water-based paint formulation, and also because with a greater content of solids allow to get more visible differences in the viscosity tests.

On the other hand, with a high value of solid contents, the suspensions become opaque due to the amount of TiO_2 particles. This effect does not allow a good measurement of DLS

due to the large number of particles in suspension, making difficult the measurement of the particles size, since the equipment cannot distinguished two particles that are too close.

4. Results and Discussion

4.1. Characterization of the macro initiators and block copolymers

Table 1 summarizes the characterization of the different (co)polymers prepared in this work as well as the reaction time.

Table 1 – M_n and M_w/M_n values determined by GPC and M_n value determined by ^{1}H NMR, for the synthetized polymers.

Block Copolymer	Target DP	Reaction time (h)	Monomer conversion (%)	$M_{n,GPC}$ (g/mol)	M_w/M_n (PDI)	$M_{n,NMR}$ (g/mol)
mPEG$_{113}$-*b*-PDMAEMA$_{44}$	90	0.92	49.1	25,422	1.32	18,121
mPEG$_{45}$-*b*-PDMAEMA$_{38}$	90	0.75	42.3	8,959	1.33	8,057
mPEG$_{113}$-*b*-P4VP$_{55}$	200	1.92	25.8	19,787	1.32	10,902
mPEG$_{45}$-*b*-P4VP$_{31}$	50	3	72.4	8,864	1.28	8,368
PtBA$_{37}$	50	6.5	80.4	2,306	1.27	4,886
PAA$_{26}$-*b*-P4VP$_{30}$	100	1.52	29.5	17,949	1.70	8,039
PtBA$_{41}$	50	6.5	77.4	2,366	1.26	5,362
PAA$_{41}$-*b*-PDMAEMA$_{56}$	100	1.22	49.6	16,006	1.70	14,208
mPEG$_{113}$-*b*-PtBA$_{12}$	80	1.83	23.1	9,975	1.09	3,666

The size of the segments of each block copolymer was determined by respective ^{1}H-NMR. Since the mPEG macroinitiator used already has known number of repeating units, the ^{1}H-NMR spectrum was mainly used to confirm the success of functionalization using CPC or BBiB, Cl or Br functional group, respectively. A typical ^{1}H-NMR spectrum for mPEG-Br is presented in Figure 10, while the ^{1}H-NMR spectrum for mPEG-Cl is presented in Figure I-1 (Appendix I), with the assigned peaks. For mPEG-Br, Figure 10, the bromoisobutyryl terminal group had a unique 1H NMR peak at 1.94 ppm due to its six protons, and comparing the intensity of this peak with that of ethylene proton peak at 3.5 ppm, the conversion of mPEG-OH into mPEG-Br is confirmed (Martinez-Castro, Zhou et al. 2010).

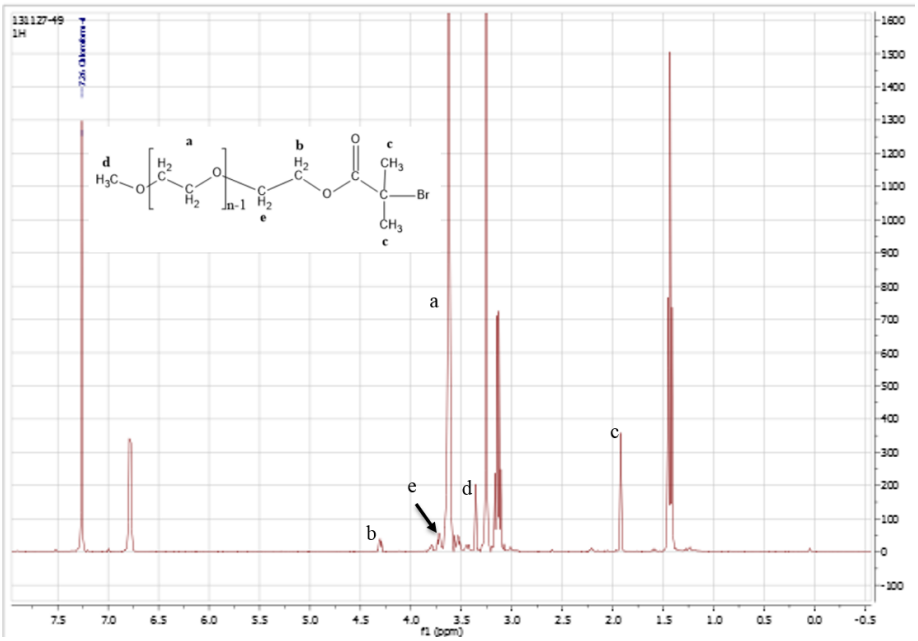

Figure 10 – ^{1}H-NMR spectra of mPEG-Br in $CDCl_3$ and molecular structure.

Similarly, for mPEG-Cl (Figure I-1, Appendix I) the confirmation can be done through comparison of the integrated peak at 1.7 ppm due to its three protons with the ethylene proton peak at 3.5 ppm.

For $mPEG_{113}$-*b*-$PDMAEMA_{44}$ copolymer, the methylene protons (CH_3O-) from the mPEG initiator at about 3.3 ppm can be observed in Figure 11 which allowed to determine the number of PDMAEMA repeating units and posterior number-average molecular weight. On the basis of the integral ratio of peaks *g*, corresponding to initiator chain, and peak *e*, it is possible to estimate the repeating unit number, of DMAEMA monomer. The same procedure is also performed for $mPEG_{45}$-*b*-$PDMAEMA_{38}$ (Figure I-2, Appendix I).

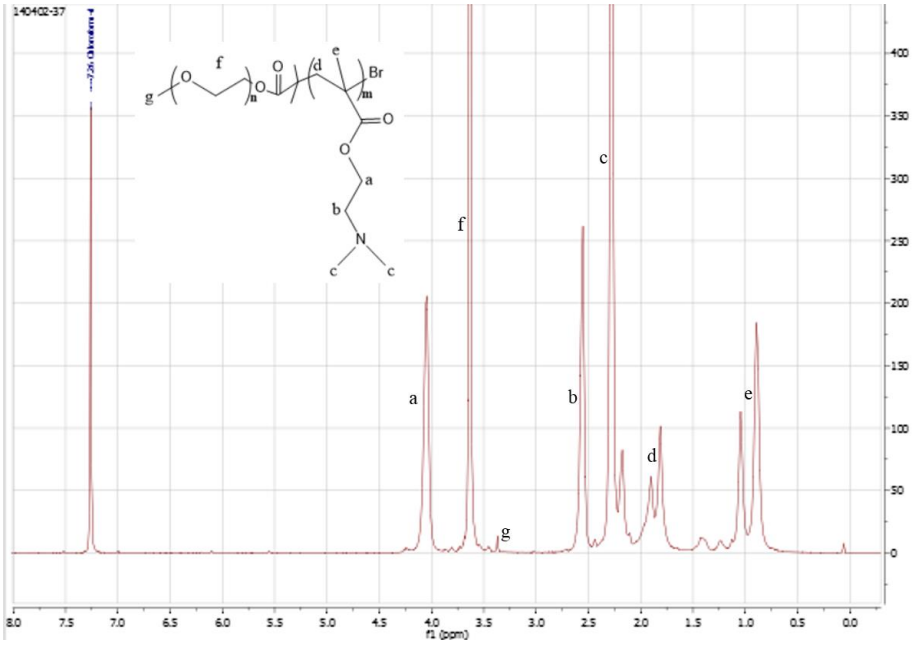

Figure 11 – ^{1}H-NMR spectra of mPEG$_{113}$-*b*-PDMAEMA$_{44}$ in $CDCl_3$ and molecular structure.

The composition of PEG-*b*-P4VP is determined by the ratio of the total area of peaks *g* and *f*, corresponding to pyridine ring, to peak *a* (Figure II-1 and Figure II-2, Appendix II) (Wang, Zhao et al. 2010).

In the case of PtBA, DP was estimated integrating the peak *a*, corresponding to the (CH_3O-) group which belongs to the initiator, and peak *b* or *c* (Figure III-1, Appendix III).

Similarly to PEG-*b*-P4VP and PEG-*b*-PDMAEMA, the DP of PtBA-*b*-P4VP and PtBA-*b*-PDMAEMA (Figure III-2, Appendix III and Figure IV-1, Appendix IV respectively) is calculated integrating the same peaks of PDMAEMA and P4VP blocks, but taking as reference the peak *a*, corresponding to the PtBA macroinitiator. After hydrolysis of PtBA group into PAA, PAA-*b*-P4VP was analyzed in DMSO and in acidic D_2O. As can be seen, in Figure 12, the characteristic groups of the pyridine group are visible, peak *h* and *g*.

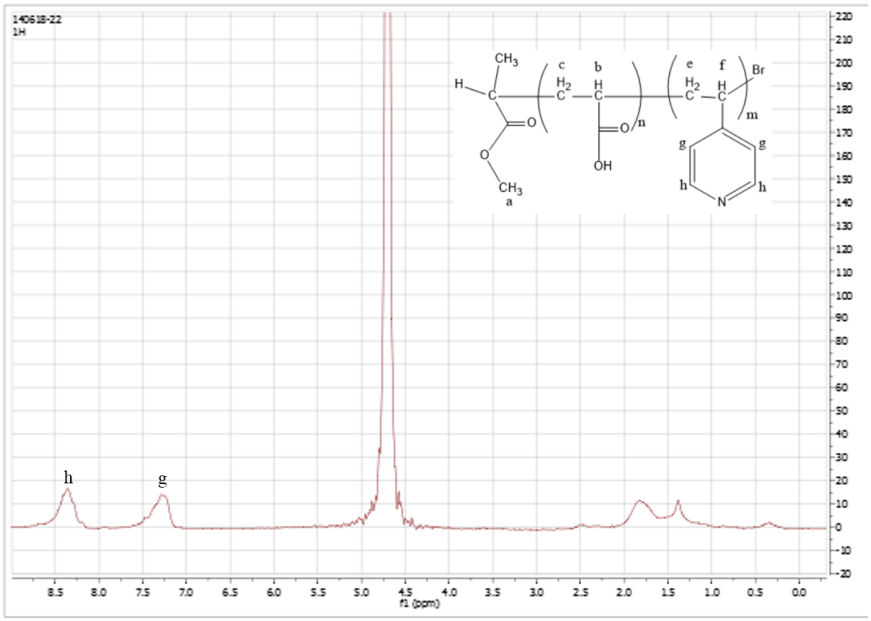

Figure 12 – ^{1}H-NMR spectra of PAA_{26}-*b*-$P4VP_{30}$ in D_2O at pH = 2, and molecular structure.

In Figure 12, the characteristic peaks corresponding to (-CH_2-) and (-CH-) groups, belonging both to PtBA and PAA groups cannot be distinguished. For this reason, the block copolymer was analyzed in DMSO (Figure 13), where the peaks of (-CH_2-) and (-CH-) corresponding to *c* and *d*, respectively, can be observed, and in its turn the peaks corresponding to pyridine ring become less intense.

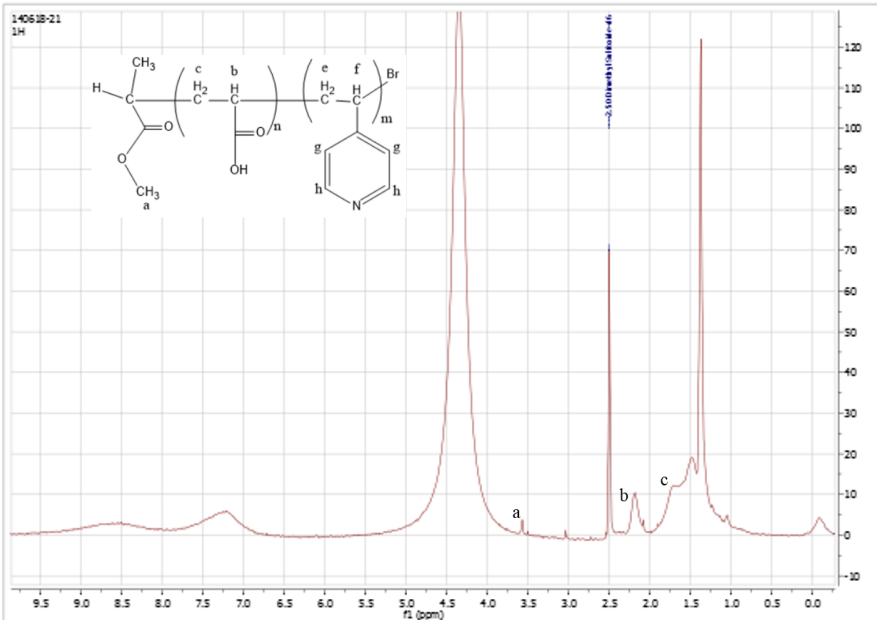

Figure 13 – ^{1}H-NMR spectra of PAA_{26}-*b*-$P4VP_{30}$ in DMSO and molecular structure.

Comparing the peak at 1.44 ppm, ascribed to the methyl protons of tBA units in Figure III-2 and Figure 13, a decreasing intensity is observed, which suggests that the esther groups of PtBA were partly hydrolyzed. The degree of hydrolysis is determined by the ratio of the peak areas, at 1.44 ppm, after and before hydrolysis (Zhang, Ai et al. 2011), and for this copolymer it was found to be approximately 70%. Contrary to what was observed for PAA-*b*-P4VP, the peaks corresponding to PDMAEMA block and PtBA are both visible in the DMSO ^{1}H NMR (Figure IV-1 and Figure IV-2, Appendix IV). After hydrolysis reaction, the peak at 1.44 corresponding to the methyl protons of tBA units are not very clear, suggesting that tBA units were fully hydrolyzed.

For $mPEG_{113}$-*b*-$PtBA_{12}$ characterization, the peak at 3.3 ppm from the mPEG initiator was used as reference to calculate the number of PtBA units, through integration of the peak *d* (Figure V-1, Appendix V). After hydrolysis, the ratio between peaks *a* and *f* (Figure V-2, Appendix V) remained very similar to the corresponding peaks before the hydrolysis, which indicates that the reaction was not effective.

As mentioned earlier, the main objective of this work was the stabilization of TiO_2 particles by using amphiphilic copolymers aiming to provide steric and/or electrostatic stabilization. The copolymers synthesized and used over the stabilization studies are mainly amphiphilic, where blocks of PEG and PAA (Xiao, Chen et al. 2013) are hydrophilic, while those composed by P4VP (Creutz and Jérôme 1999; Rocha, Mendes et al. 2014), PtBA and PDMAEMA (Zhang, Ai et al. 2011) are hydrophobic. These two hydrophobic groups were used with of the purpose to interact with the TiO_2 particles, through attachment into the particles surface and by that means ensure their stabilization. Depending on the pH, P4VP may be protonated or not, which influence its solubility in water. Since the pH used in this work was always adjusted to be around 9.5, P4VP would be deprotonated and thus water insoluble (Creutz and Jérôme 1999). Hence, block copolymers formed by PEG-*b*-P4VP and PAA-*b*-P4VP will form micelles with a P4VP core and PEG or PAA corona. The adsorption of P4VP segment into pigment surface is believed to be due to the hydrogen bonding (Creutz and Jérôme 1999) that is established between the hydrogens bonded to the N group of vinyl pyridine rings, and the hydrogens from the Al-OH groups covering the titania surface (Farrokhpay 2009). At the pH used, PAA group is an anionic polyelectrolyte (Bo and Zhao 2006), which implies the ionization of the acrylic acid repeat units (COOH into COO-) providing intermolecular electrostatic repulsive interactions (Zhang, Ai et al. 2011). Therefore, for the PEG-*b*-P4VP copolymer the stabilization mechanism expected is based on

steric interactions, while for the PAA-*b*-P4VP copolymer the stabilization mechanism will mostly based on steric and electrostatic interactions.

PDMAEMA has a temperature and pH responsive character, but for a neutral or a alkaline medium is water insoluble (Zhang, Ai et al. 2011). As in the case of P4VP, PDMAEMA block anchors to the alumina coated TiO_2 due to hydrogen bonding and Lewis acid-base interactions (Creutz and Jérôme 2000).

Although the PEG-*b*-PtBA hydrolysis reaction has not occurred as expected, this block copolymer was also used for the stabilization tests due to its amphiphilic nature. The objective of this attempt was to evaluate if the interaction between the PtBA segment and the alumina surface of titania particles was possible, since from theoretical standpoint the block copolymer composed by PEG-b-PtBA must form micelles with a PtBA core and a PEG corona.

In most of polymers used, their molecular weights are below of 20,000 g/mol because according to Farrokhpay (Farrokhpay 2009) this is the preferred weight for polymeric dispersants, while above 10^6 g/mol the polymers are suitable to be mainly used as flocculants. In fact, polymeric dispersants just need a molecular weight which provides an enough polymer length to overcome van der Waals forces of attraction between pigment particles. With this aspect in mind, two PEG block chains with different lengths were used both with P4VP as PDMAEMA, in order to evaluate the influence of the hydrophilic segment in the pigments stabilization. In the other hand, when the polymeric chains are too long, they have a high potential to cause a particle-particle bridging, causing flocculation, and posteriorly, a reduction in the dispersion performance. Other possibility with too long chains polymers is the tendency of them to fold back onto themselves (Farrokhpay 2009).

4.2. Dynamic Light Scattering (DLS)

DLS study was performed in order to evaluate the effectiveness of copolymers to stabilize TiO_2 particles, through measurement of the hydrodynamic diameter (D_h). Also a visual image assessment of the particles stabilization can be done through Figure 15 (Page 42). The evolution of this parameter was measure during 12 days, and the results are presented in Table 2.

Table 2 – D_h and PDI values for self-assemble of the copolymers in study in the presence of TiO_2 particles for several days, as determined by DLS.

Block Copolymer	Day 0		Day 1		Day 2		Day 5		Day 7		Day 9		Day 12	
	Z-average		Z-average		Z-average		Z-average		Z-average		Z-average		Z-average	
	$D_{h,intensity}$ (nm)	PDI	$D_{h,intensity}$ (nm)	PDI	$D_{h,intensity}$ (nm)	PDI	$D_{h,intensity}$ (nm)	PDI	$D_{h,intensity}$ (nm)	PDI	$D_{h,intensity}$ (nm)	PDI	$D_{h,intensity}$ (nm)	PDI
$mPEG_{113}$-*b*-$PDMAEMA_{44}$	797,00	0,47	263,50	0,23	287,00	0,30	230,90	0,32	223,20	0,38	190,40	0,39	198,30	0,38
$mPEG_{45}$-*b*-$PDMAEMA_{38}$	564,30	0,43	241,60	0,13	237,60	0,14	189,40	0,21	189,90	0,22	182,80	0,19	190,00	0,23
$mPEG_{113}$-*b*-$P4VP_{55}$	554,20	0,15	266,80	0,31	164,70	0,55	78,99	0,70	68,47	0,61	61,77	0,56	47,61	0,60
$mPEG_{45}$-*b*-$P4VP_{31}$	406,20	0,14	270,90	0,13	191,50	0,27	242,30	0,46	113,30	0,64	99,91	0,67	94,58	0,66
PAA_{26}-*b*-$P4VP_{30}$	932,60	0,15	367,70	0,24	376,00	0,21	378,00	0,39	309,90	0,36	350,30	0,43	263,30	0,44
PAA_{41}-*b*-$PDMAEMA_{56}$	533,00	0,16	302,70	0,07	246,20	0,08	230,00	0,14	223,90	0,18	218,20	0,12	212,80	0,15
$mPEG_{113}$-*b*-$PtBA_{12}$	824,60	0,18	198,70	0,57	125,50	0,24	90,04	0,25	86,93	0,21	84,02	0,19	83,47	0,16
Additol	367,20	0,14	256,70	0,08	210,00	0,06	307,10	0,23	183,50	0,07	178,80	0,17	190,10	0,19
TiO2	921,30	0,47	283,10	0,28	334,10	0,38	548,50	0,45	496,50	0,46	520,50	0,54	488,90	0,51

In Table 2, for the PDI values presented in day 0, it can be observed that for most copolymers this value is small and comparable to the Additol sample, indicating a narrow particles size distribution. PAA_{41}-*b*-$PDMAEMA_{56}$ is the only sample which exhibits PDI and D_h values that not have a large variation from the 1st day until the end of the test, indicating a very good stabilizations of the particles and particles size distribution. Furthermore, this sample shows better values than Additol, which after 7th day shown no stabilized particles in solution, since the measured diameters are below of 220 nm, the mean size of TiO_2 particles.

Also PAA_{26}-*b*-$P4VP_{30}$ presents values that allow to conclude a good TiO_2 particles stabilization, although with a larger particles size distribution.

A measurement of the micelles hydrodynamic diameter without a presence of TiO_2 particles was taken, to further comparison with the diameters obtained in the presence of the particles. The hydrodynamic diameters are summarized in Table 3 while the evolution at several days, of their hydrodynamic diameter in the presence of TiO_2 particles can be evaluated in Figure 14 and Figure 16.

Table 3 – D_h and PDI values of aqueous block copolymer dispersions, as determined by DLS.

Block Copolymer	Z-average $D_{h,intensity}$ (nm)	PDI
$mPEG_{113}$-*b*-$PDMAEMA_{44}$	170,2	0,425
$mPEG_{45}$-*b*-$PDMAEMA_{38}$	849,8	0,502
$mPEG_{113}$-*b*-$P4VP_{55}$	26,26	0,321
$mPEG_{45}$-*b*-$P4VP_{31}$	22,16	0,316
PAA_{26}-*b*-$P4VP_{30}$	384,1	0,487
PAA_{41}-*b*-$PDMAEMA_{56}$	566,2	0,474
$mPEG_{113}$-*b*-$PtBA_{12}$	1191	0,331
Additol	547,6	0,542

For different samples “day 0” was considered time after the samples were taken to remove the polymer solvent.

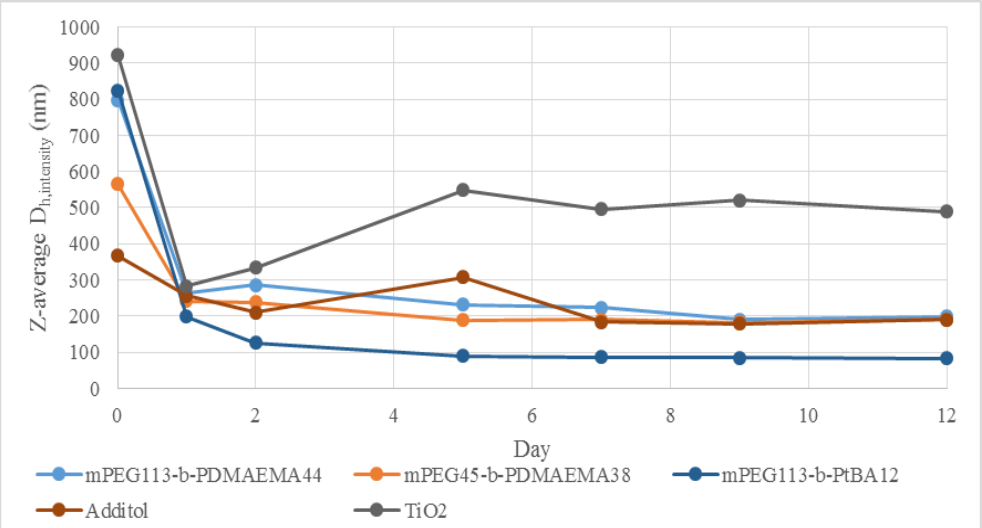

Figure 14 – Hydrodynamic diameter of mPEG$_{113}$-*b*-PDMAEMA$_{44}$, mPEG$_{45}$-*b*-PDMAEMA$_{38}$, mPEG$_{113}$-*b*-PtBA$_{12}$ and Additol in the presence of TiO_2 particles, and TiO_2 particles, at pH=9.5 and during a few days.

From Figure 14, it is possible to observe that in day 0 all samples exhibit hydrodynamic diameters well above of the 220 nm of the initial TiO_2 particles size, with the exception of commercial polymer. Such fact could indicate that the amount of polymer was insufficient to stabilize the TiO_2 particles, being the diameter measured a result of flocculation between the particles. In this view, the interaction between particles and the polymer available in the formulation was not enough to afford and efficient stabilization.

It is visible that the sample of mPEG$_{113}$-*b*-PtBA$_{12}$ is one that has the worst result, with a particles mean size below 200 nm after the 1st, when the average size of TiO_2 particles is 220 nm. This result indicates that for this block copolymer the TiO_2 particles flocculated and the sizes measured might correspond to self-assembly structures. This assumption can be confirmed by Figure 15 where the samples with TiO_2 particles and TiO_2 particles stabilized by mPEG$_{113}$-*b*-PtBA$_{12}$, show a similar behavior.

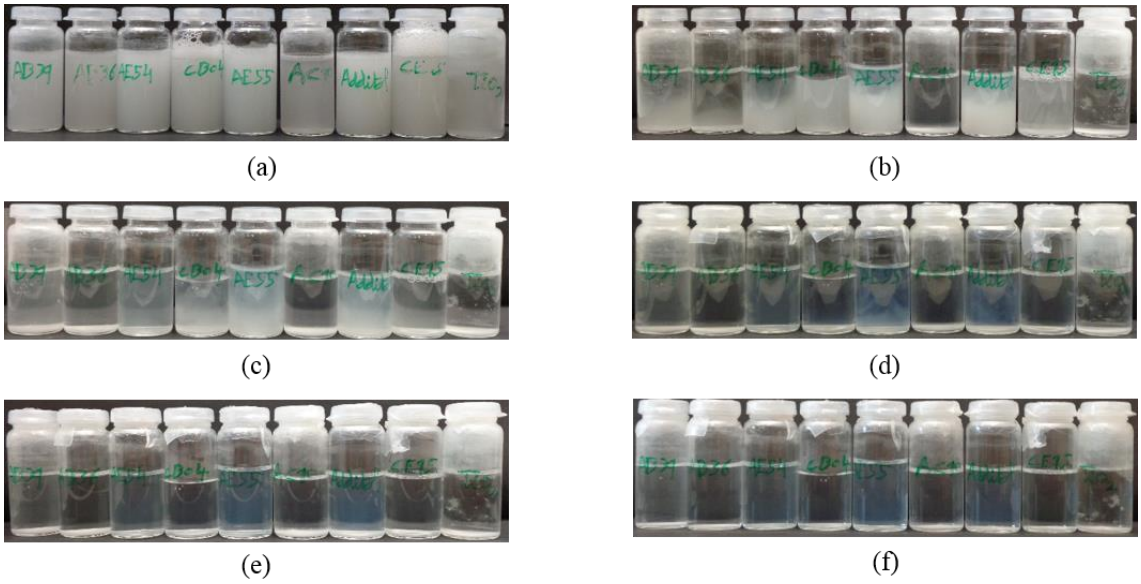

Figure 15 – Photos of TiO_2 suspensions on (a) day 0, (b) day 1, (c) day 2, (d) day 5, (e) day 7, and (f) day 9. From right to the left the samples are: $mPEG_{45}$-*b*-$PDMAEMA_{38}$, $mPEG_{113}$-*b*-$PDMAEMA_{44}$, $mPEG_{113}$-*b*-$P4VP_{55}$, PAA_{41}-*b*-$PDMAEMA_{56}$, $mPEG_{45}$-*b*-$P4VP_{31}$, $mPEG_{113}$-*b*-$PtBA_{12}$, Additol VXW 6200, PAA_{26}-*b*-$P4VP_{30}$ and TiO_2.

It can be seen that mostly of the particles are deposited in the flask's bottom, after the first day. For the TiO_2 sample there is a notorious decay in D_h from the starting to the first day, which can be caused by the sedimentation of large clusters of particles, and posterior an increase of the diameter due to the formation of new clusters from the remaining particles in suspension. Despite the visual evaluation indicate do not have particles in suspension in both samples after the first day, by the DLS analysis is it possible to see that in TiO_2 sample there are particles in suspension, more specifically clusters with a size range of 500-600 nm from 5^{th} day to 12^{th} day. A different behavior has found to $mPEG_{113}$-*b*-$PtBA_{12}$ sample, where diameters below 220 nm remained from the starting day to the end of the analysis. This result can imply that bridging flocculation is present, and instead of stabilize TiO_2 particles, the copolymers is acting as a precipitation agent, despite small molecular weight and hydrophobic chain.

The samples of based on mPEG-*b*-PDMAEMA behave similarly, with a decreasing in the hydrodynamic diameter until values of ~200 nm, but with the $mPEG_{113}$-*b*-$PDMAEMA_{44}$ sample showing values slightly higher than $mPEG_{45}$-*b*-$PDMAEMA_{38}$ in the initial times which can be explained by the fact of the higher hydrophilic segment of $mPEG_{113}$-*b*-$PDMAEMA_{44}$. With such result, and also similar to that verified by Additol, seems that mPEG-b-PDMAEMA sample are capable to stabilize TiO_2 particles in an aqueous medium.

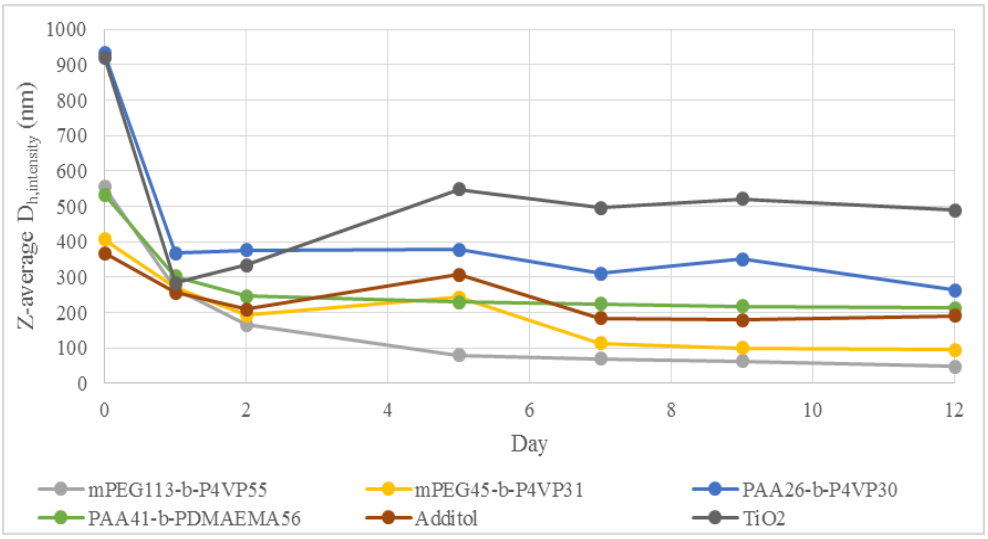

Figure 16 – Hydrodynamic diameter of mPEG$_{113}$-*b*-P4VP$_{55}$, mPEG$_{45}$-*b*-P4VP$_{31}$, PAA$_{26}$-*b*-P4VP$_{30}$, PAA$_{41}$-*b*-PDMAEMA$_{56}$ and Additol in the presence of TiO_2 particles, and TiO_2 particles, at pH=9.5 and during a few days.

From Figure 16, it is possible to observe that both mPEG$_{113}$-*b*-P4VP$_{55}$ and mPEG$_{45}$-*b*-P4VP$_{31}$ form interactions with TiO_2 particles, which is visible from the increase on D_h. These interactions can be confirmed taking into account that the size of the block copolymers in solution increased from ~26 nm (see Table 3) to values around ~400 nm for mPEG$_{45}$-*b*-P4VP$_{31}$ and ~554 nm for mPEG$_{113}$-*b*-P4VP$_{55}$. In the first day, samples appear to have particles stabilized by the copolymer, with diameter above 220 nm, but after that, these samples have the tendency to decrease the particles diameter, and starting of the 7th day, the result is inferior to the Additol, what means that particles started to sediment. Similarly to what happens with PEG-b-PDMAEMA, the sample with mPEG$_{113}$-*b*-P4VP$_{55}$ has a higher diameter than mPEG$_{45}$-*b*-P4VP$_{31}$ due to the hydrophilic segment length. Although the weak performance of these samples, they are better than those analyzed previously, in Figure 14.

The sample of PAA$_{26}$-*b*-P4VP$_{30}$ after the first analyze, presented a similar hydrodynamic diameter with the sample only with TiO_2 particles, but since 1st day until 12th day the diameter measured was in the range of 300 and 400 nm. A reasonable explanation for this fact is the insufficient amount of copolymer to stabilize all particles present in the sample, which took to the formation of TiO_2 aggregates, even during vigorous agitation that samples were subject overnight. After the first measure, the aggregates deposited, while in suspension the stabilized particles remained.

PAA$_{41}$-*b*-PDMAEMA$_{56}$ sample, between day 0 and 2, verifies the same phenomena than in the other samples, corresponding to the deposition of the bigger particles which probably were not fully stabilized by the copolymer. After that period, the tendency of the

particles diameter is persist almost unchanged, as shown in Figure 16 and better viewed in Table 2.

After this first analysis for the results of DLS measures, seems that samples with PAA as hydrophilic segment presents a more effective and durable stability of the TiO_2 particles, when compared with the mPEG segment, once the samples of PAA_{26}-*b*-$P4VP_{30}$ and PAA_{41}-*b*-$PDMAEMA_{56}$ shown more interesting results than the mPEG-*b*-P4VP and mPEG-*b*-PDMAEMA, respectively, with both a longer and a shorter mPEG chain length. This result indicates that the electrostatic barrier provided by the PAA segment seems more effective against flocculation than only the steric barrier provided by mPEG segment, not counting with the effect of hydrophobic segment, that are very similar in the case of the polymers with mPEG and PAA segment. Through comparison of the different copolymers in Figure 15, the two that stand out are PAA_{26}-*b*-$P4VP_{30}$ and PAA_{41}-*b*-$PDMAEMA_{56}$, in which the second one seems to be very promising, since is the sample which exhibit diameters compatible with particles dispersion efficiency, longer than Additol, and the PDI values are lower and comparable to those of Additol, meaning a short range of diameters distribution, formed by the complex copolymer/TiO_2 particles.

4.3. Zeta potential measurement

Zeta potential measurements were performed for the different block copolymers (Figure 17) and mixtures of those with TiO_2 particles (Figure 18). The results obtained are summarized in Table VII-1 and Table VIII-1 (Appendix VII and Appendix VIII) and plotted in Figure 12 and Figure 13.

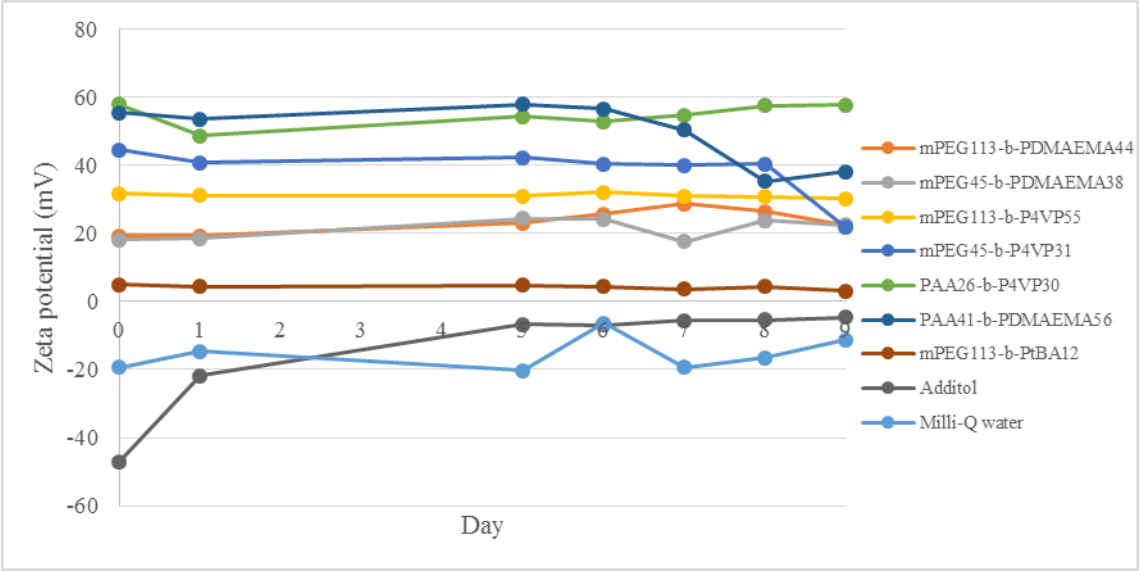

Figure 17 – Variation of zeta potential of the different block copolymers suspensions.

The ς potential measurements for the block copolymers solutions were performed in order to serve as a basis to the measurements to the samples with TiO_2 particles. As can be seen from Figure 17, some samples present variations in this parameter over the time. Indeed, the commercial dispersant is the one that shows the highest variation in the measured values, However, when these dispersants are mixed with TiO_2 particles, the values of ς potential are practically unchanged along the time, as illustrated by Figure 18.

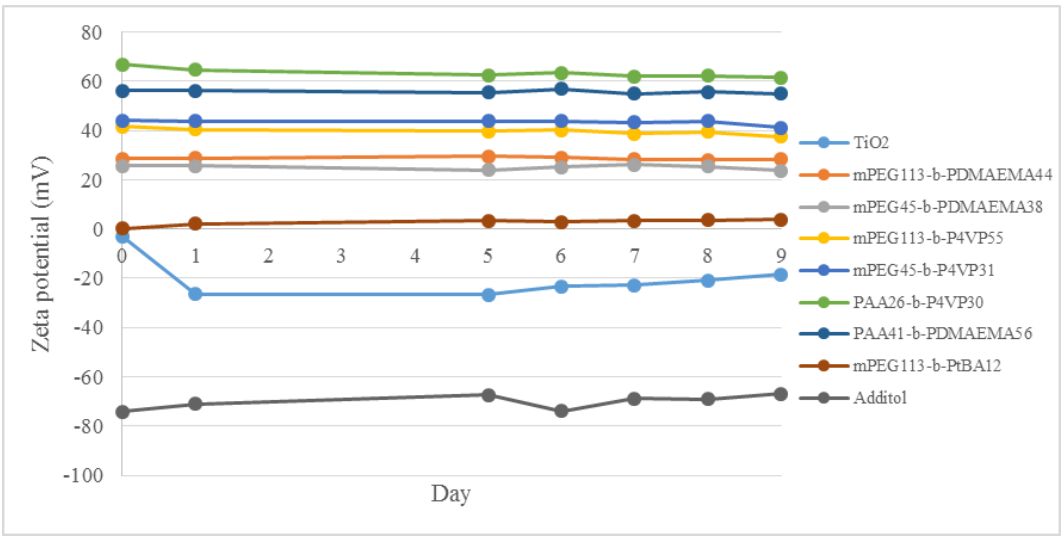

Figure 18 – Variation of zeta potential of TiO_2 suspensions with block copolymers as stabilizers.

It is known that for highly negative or positive values of potential zeta (higher than 30 mV in module), the particles in dispersion tend to repel each other (Mandzy, Grulke et al.

2005). This means that an electrostatic stabilization is present, and contributes to the prevention of flocculation.

The two samples of mPEGx,y-*b*-PDMAEMAz,w (x=113, y=45 and z=44, w=38) and the sample of $mPEG_{113}$-*b*-$PtBA_{12}$, are not in the values range referred previously, which imply that the possible stabilization mechanism which could prevent the particles agglomeration would be based only on steric effect. For $mPEG_{113}$-*b*-$PtBA_{12}$ this mechanism showed to be not effective, as seen in DLS analysis (see Section 4.2). Taking into account the data of DLS and ς potential measurements obtained for $mPEG_{113}$-*b*-$PtBA_{12}$, it can be concluded that steric effect provided are not sufficient to overcome the attraction forces of Van der Waals, leading to the agglomeration of the titania particles.

Samples with mPEG-P4VP have a very identical behavior, yet their values are a little different, which may be due to chain length of mPEG segment. A possible cause can be due to the slightly higher segment of mPEG segment, which will interfere in the charge interaction. Based on pH used, the P4VP segment was expected to be deprotonated, however through analysis of Figure 18 it can be seen that samples with P4VP in micellar core show a relatively high potential zeta, which means that most probably the full deprotonatation of this segment was not achieved. This observation can be due to the fact of the P4VP chain is not fully adsorbed in the particles surface, which allows a partially protonation of some P4VP groups, providing by this means an electrostatic stabilization. Also this effect can be ascribed to changes on the pH samples across the time. A full understanding of the mechanism that justifies the obtained results would require additional experiments.

The samples of PAA_{26}-*b*-$P4VP_{30}$ and PAA_{41}-*b*-$PDMAEMA_{56}$ are those who present the higher ς potential, indicating a high effect of electrostatic mechanism in the system. This result corroborates the ionization of the acrylic acid repeat units.

4.4. Rheological measurements

In the rheological measurements the parameter in study was the viscosity of the TiO_2 suspensions stabilized with the different polymeric dispersants, and values were measured from supernatant of each sample. The viscosities values, both for samples of polymeric dispersants in aqueous solutions, and samples of polymeric dispersant with TiO_2 particles are present in Table IX-1 and Table IX-2 (Appendix IX).

The evolution of the samples viscosity can be observed in Figure 19 and Figure 20.

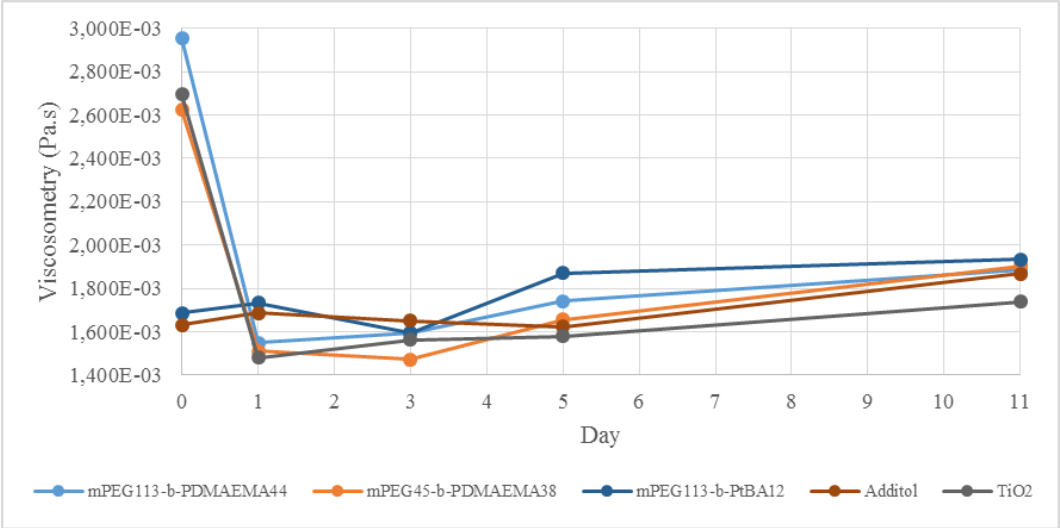

Figure 19 – Viscosity of $mPEG_{113}$-*b*-$PDMAEMA_{44}$, $mPEG_{45}$-*b*-$PDMAEMA_{38}$, $mPEG_{113}$-*b*-$PtBA_{12}$ and Additol in the presence of TiO_2 particles at a few days.

From Figure 19, it can be observed that the sample containing only TiO_2 particles exhibit the second highest viscosity, which drops abruptly after one day and then maintains approximately constant. This result indicates that most part of TiO_2 agglomerates precipatates only after one day, which is confirmed by the photos presented in Figure X-1 (Appendix X).

Both samples with the mPEG-b-PDMAEMA, have a high viscosity in day zero and a fast decrease after that, indicating that in both samples there is a high deposition of the particles, and therefore, they are not good stabilizers for TiO_2 particles. This result is also confirmed in Figure X-1 (Appendix X), where the two samples exhibit two distinct phases: the inferior phase corresponding to the TiO_2 particles flocculation and their posterior sedimentation, while superior phase is almost transparent, indicating that only a residual amount titania pigment is present. It is also important to notice the differences between the images of PEG-b-PDMAEMA and the sample of TiO_2, especially in Figure X-1 (e) and (f) (Appendix X), where it is clearly visible a more translucent supernatant in the copolymers samples than in TiO_2 sample. Therefore, these copolymers are acting as precipitating agent and not stabilizers, as it was intended.

Contrary to expected, after analysing the results of previous tests, the $mPEG_{113}$-*b*-$PtBA_{12}$ viscosity is very low when compared with TiO_2 sample, and it has a variation along the time similarly to the commercial dispersant. This result seems to indicate that polymer could prevent titania particles flocculation, stabilizing them by a steric mechanim. Moreover,

analysing the different photos taken over the time (Figure X-1, Appendix X), and comparing the visual differences among $mPEG_{113}$-*b*-$PtBA_{12}$ sample and TiO_2 sample, it is possible to visualize that the titania particles of the $mPEG_{113}$-b-$PtBA_{12}$ sample, require more time to depositate in the bottom of flask. This conflict of results amongst viscosity and DLS, could be derived from the different proportion of copolymer:TiO_2 used in the both tests, which originate different conclusions. In the future, new tests with this copolymer should be carried out, in order to clarify the differences verified, because if in rheological tests the proportion of copolymer would be higher than the TiO_2, when compared to DLS, the final result would be understandable, once the quantity in DLS test were insufficient to stabilize the particles or to self-assembly. Such fact it is not verified, and that is why it is important to understand the phenom behind this apparent contradictory result.

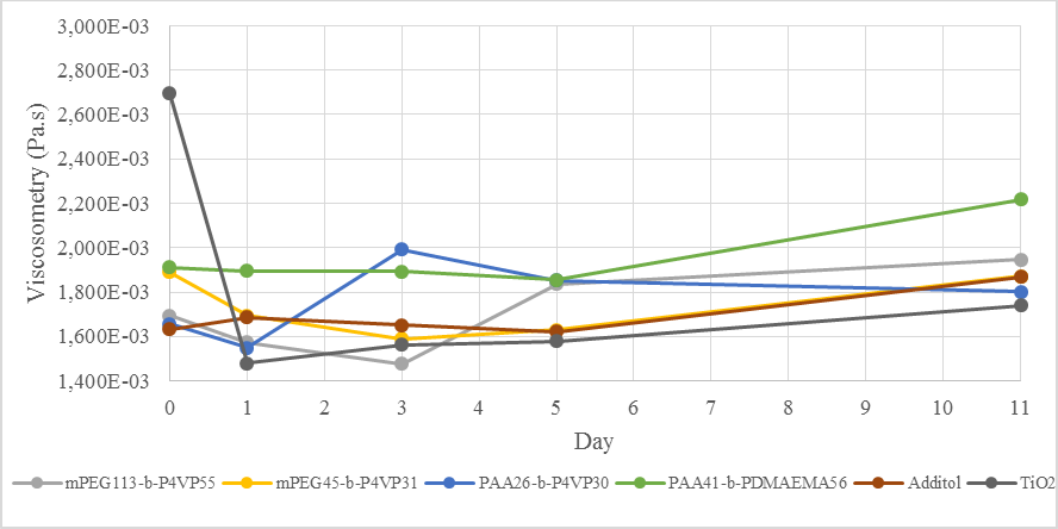

Figure 20 – Viscosity of $mPEG_{113}$-*b*-$P4VP_{55}$, $mPEG_{45}$-*b*-$P4VP_{31}$, PAA_{26}-*b*-$P4VP_{30}$, PAA_{41}-*b*-$PDMAEMA_{56}$ and Additol in the presence of TiO_2 particles at a few days.

In Figure 20, the tested copolymers show a lower viscosity in day zero than the TiO_2 sample, indicating a successful adsorption of them into particles surface, which provides a barrier against the attractive forces.

$mPEG_{45}$-*b*-$P4VP_{31}$ has a very similar performance compared to Additol, being the major difference the viscosity in day zero. Most of the copolymers tested do not present an accentuated viscosity variation, except to PAA_{26}-*b*-$P4VP_{30}$, which shows an increasing viscosity from day one to day three. After the 5^{th} day (Figure 19 and in Figure 20) the samples possess an higher viscosity, and for this reason it is important to evaluate this parameter during a longer period of time. The most notorious difference in the viscosity is verified for

PAA_{41}-*b*-$PDMAEMA_{56}$ sample, as can be seen in Figure 20, and comparing with the viscosity of the sample containing only a solution of this copolymer for the 11th day (Table IX-1, Appendix IX), the difference between them is very significant. At this stage, it is impossible to justify this result.

4.5. Paint formulation performance

In an earlier phase of this work, and in collaboration with Resiquímica, three different block copolymers were tested with its paint formulation, which is similar to that presented in Figure VI-1 (Appendix VI), and some properties were analyzed. The copolymers used were formed by a hydrophilic segment of mPEG and a hydrophobic segment PDMAEMA and P4VP, where the mPEG segment used had two different chain size for the case of the copolymer formed by P4VP. These two different chain lengths of mPEG with a very similar length of P4VP chain were used, in order to understand the influence of mPEG chain length in the dispersing of TiO_2 particles. The corresponding copolymers properties are shown in Table 4.

Table 4 – M_n and M_w/M_n values determined by GPC and M_n value determined by ^1H NMR, for the synthetized polymers used in paint formulation.

Block Copolymer	$M_{n,GPC}$ (g/mol)	M_w/M_n (PDI)	$M_{n,NMR}$ (g/mol)
$mPEG_{113}$-*b*-$PDMAEMA_{23}$	14927	1,271	8637
$mPEG_{113}$-*b*-$P4VP_{34}$	21637	1,343	8614
$mPEG_{45}$-*b*-$P4VP_{40}$	11485	1,236	6296

The performance of each copolymer was compared with the formulation used by Resiquímica using the commercial dispersing agent - Additol VXW 6200. Some of the measured characteristics used by Resíquimica to evaluate paints, are presented in Table 5.

It is important to note that the samples of paint produced were not the indicated, since the amount of copolymers was not the sufficient to perform the paint formulation correctly.

Despite this, these results can be evaluated as a starting point to understand if the copolymers used are capable to stabilize the titania pigment and offer better paint properties, than commercial dispersant. After the preparation of the paint samples with the different copolymers, and posterior application in film form to evaluate CIELab parameters, brightness and contrast ratio, it was verified the formation of some titania pigment aggregates. Such phenomenon can be due to limited amount of copolymers used in the formulation. Having this information in mind, another important factor to be studied later is the optimum amount of copolymer required to stabilize titania particles.

Table 5 – Properties of a paint formulation containing different polymers as stabilizing agent.

General properties	Additol VXW 6200	$mPEG_{113}$-*b*-$PDMAEMA_{23}$	$mPEG_{113}$-*b*-$P4VP_{34}$	$mPEG_{45}$-*b*-$P4VP_{40}$
CIELab parameter				
L	98.76	98.58	98.39	98.62
a	-0.83	-0.39	-1.06	-0.96
b	3.42	3.40	3.54	3.78
Brightness (u.b.)				
60º angle	26.7	35.4	39.8	43.8
85º angle	57.5	60.8	67.1	68.9
Contrast Ratio (%)	93.83	93.56	94.42	94.05
Initial viscosity				
ICI Cone&Plate at 25ºC (P)	1.4	3.0	1.2	1.2
Stormer at 23ºC (KU)	87	108	94	103
Brookfield at 23ºC H4, 20rpm (mPa.s)	5200	8700	6550	--
Viscosity after 14 days at 50ºC				
ICI Cone&Plate at 25ºC (P)	1.3	Gel	1.6	2.2
Stormer at 23ºC (KU)	89.4		122	135
Brookfield at 23ºC H4, 20rpm (mPa.s)	5400		22000	--
Viscosity after 28 days at 50ºC				
ICI Cone&Plate at 25ºC (P)	1.2	Gel	1.6	2.6
Stormer at 23ºC (KU)	95.7		141	>150
Brookfield at 23ºC H4, 20rpm (mPa.s)	7100		36000	--

Analyzing the chromatic coordinates from Table 5, corresponding to Lab parameters, and the contrast ratio, no significate differences between the samples can be observed. However, regarding the paint brightness, known to be an indicator of pigment distribution (since when an increase in pigment aggregate size occurs the brightness of a paint film

decreases (Farrokhpay, Morris et al. 2010)), the differences between commercial dispersant and the tested copolymers are very significant. The block copolymer $mPEG_{45}$-b-$P4VP_{40}$ presents a better performance. Therefore, it is possible conclude that the three tested dispersants are effective agents in the TiO_2 dispersion, despite of film formation reveal some aggregates which affect the brightness. The most promising result was achieved for $mPEG_{45}$-*b*-$P4VP_{40}$ sample, and comparing with its homologous sample ($mPEG_{113}$-*b*-$P4VP_{34}$), seems that mPEG chain length can justify the difference obtained. With a smaller mPEG chain length, TiO_2 particles have the possibility to be closer to each other, without agglomeration due to the steric barrier provided by both the mPEG and the P4VP segments, and such approximation allows to have more TiO_2 particles by area unit than in the $mPEG_{113}$-*b*-$P4VP_{34}$ case, resulting in a better gloss. Therefore, it can be concluded that there are major two factors that should be taken into consideration in development of block copolymers for the TiO_2 particles stabilization: a hydrophobic segment size needed to adsorb onto the particle surface and provide a barrier against flocculation; and one hydrophilic segment large enough to disperse the particles and also provide a barrier against flocculation, and at the same time should be small enough to allow having the maximum number of particles per unit of area, providing better paint gloss.

Relative to the viscosity results were surprising due to the large variation in the values obtained. For$mPEG_{113}$-*b*-$PDMAEMA_{23}$ sample it was impossible to measure its viscosity for the 14^{th} day and 28^{th} day, because the sample turned into gel. In future studies, it is necessary to evaluate the viscosity variation of PEG-*b*-P4VP during a larger period of time, since it was the dispersant that exhibited the best brightness. It is also crucial to determine the viscosity that can be achieved maintaining the system stable.

Conclusions

Block copolymers of $mPEG_{113}$-*b*-$PDMAEMA_{44}$, $mPEG_{45}$-*b*-$PDMAEMA_{38}$, $mPEG_{113}$-*b*-$P4VP_{55}$, $mPEG_{45}$-*b*-$P4VP_{31}$, PAA_{26}-*b*-$P4VP_{30}$, PAA_{41}-*b*-$PDMAEMA_{56}$, and $mPEG_{113}$-*b*-$PtBA_{12}$, in with different hydrophobic and hydrophilic segments, were synthetized, and its effect in the TiO_2 pigments stabilization and dispersion in aqueous solution was investigated using DLS, ς potential and viscosity measurements. Furthermore, block copolymers of mPEG-PDMAEMA and mPEG-P4VP, where two sizes of mPEG chain were used in the P4VP copolymer, were analyzed in a paint formulation through CIELab parameter, brightness, contrast ratio and storage stability, using the viscosity as parameter of comparison.

The results from DLS and ς potential, of the synthesized copolymers, were compared and was possible to verify that, globally, the block copolymers of PAA_{41}-*b*-$PDMAEMA_{56}$ and PAA_{26}-*b*-$P4VP_{30}$ were those that present a better performance. In the DLS measure they exhibit hydrodynamic diameters between 200 and 400 nm, reasonably stable during 12 days, indicating a successful formation of micelles with TiO_2 particles stabilized in the core, and from ς potential was possible to check that they are the two which have a better electrostatic stabilization, from other copolymers that were synthesized. On the other hand, $mPEG_{113}$-*b*-$P4VP_{55}$, $mPEG_{45}$-*b*-$P4VP_{31}$ and $mPEG_{113}$-*b*-$PtBA_{12}$ showed the worst results, unable to stabilize the particles during the 12 days. From ς potential was possible confirm that $mPEG_{113}$-*b*-$PDMAEMA_{44}$, $mPEG_{45}$-*b*-$PDMAEMA_{38}$ and $mPEG_{113}$-*b*-$PtBA_{12}$ do not provide an effective electrostatic barrier to overcome the attraction forces of Van der Waals.

The viscosity analysis showed the incapability of mPEG-*b*-PDMAEMA in stabilize TiO_2 particles, showing a viscosity similar to the aqueous sample of titania particles, in the first measure, indicating the presence of clusters in the sample. Such inefficiency was also proved by the photos taken from the suspensions, (Figure X-1, Appendix X), contradicting the results obtained by DLS, while the other tested samples presented lower viscosities than TiO_2 sample, an indicator of dispersion and stabilization of the particles. It was also possible to verify, in the generality of samples, an increase in viscosity along the days, and a surprising result, contradicting DLS, with a good stabilization by $mPEG_{113}$-*b*-$PtBA_{12}$, as showed by Figure X-1. Such result can be due to the different proportions of copolymer: TiO_2 particles used in DLS and in the viscosity measurements, indicating that is important to study the optimum amount of copolymer used to stabilize titania particles.

The $mPEG_{113}$-*b*-$PDMAEMA_{23}$, $mPEG_{113}$-*b*-$P4VP_{34}$ and $mPEG_{45}$-*b*-$P4VP_{40}$ copolymers were used in a paint formulation and characterized according to the parameters used by Resiquímica. In these results, despite film present some clusters and the amount of each copolymer not be the necessary to perform a good paint formulation, the tested copolymers presented better brightness results than those present by commercial dispersant, an indicator of better particles dispersion. The drawback of these copolymers was the storage stability test, where the viscosity increase was large in the three samples, and even with a gel formation in the $mPEG_{113}$-*b*-$PDMAEMA_{23}$ sample. The bigger value of the $mPEG_{45}$-*b*-$P4VP_{40}$ in brightness test, than $mPEG_{113}$-*b*-$P4VP_{34}$, suggests the possibility to have bigger values with shorter peg chains, which allow more stabilized particles per unit of area, but it is a sufficiently large chain to provide a steric stabilization to prevent formation of clusters and posterior flocculation.

5. Future Works

In future work, it would be important to analyze with more detail the use of $mPEG_{113}$-*b*-$PtBA_{12}$ as dispersant, trying to understand its potential in the TiO_2 dispersion, since the results obtained for DLS and viscosity were contradictory. A TEM analysis could be a good way to evaluate if this polymer is forming micelles around the titania particles, and also to confirm if micelles formation with the other polymers used throughout the work is verified or not. Other information that can be given by TEM analysis is the present agglomerates of particles and the quality of the particle dispersions.

With the copolymers of PAA_{26}-*b*-$P4VP_{30}$ and PAA_{41}-*b*-$PDMAEMA_{56}$, which presented the most interesting results regarding DLS, ς potential and lower viscosity, would be important to evaluate their performance in a paint formulation using standard industrial procedures.

6. References

Bo, Q. and Y. Zhao (2006). "Double-hydrophilic block copolymer for encapsulation and two-way pH change-induced release of metalloporphyrins." Journal of Polymer Science Part A: Polymer Chemistry **44**(5): 1734-1744.

Braunecker, W. A. and K. Matyjaszewski (2007). "Controlled/living radical polymerization: Features, developments, and perspectives." Progress in Polymer Science **32**(1): 93-146.

Buxbaum, G. and G. Pfaff (2005). Industrial Inorganic Pigments, Wiley.

Ciampolini, M. and N. Nardi (1966). "Five-Coordinated High-Spin Complexes of Bivalent Cobalt, Nickel, andCopper with Tris(2-dimethylaminoethyl)amine." Inorganic Chemistry **5**(1): 41-44.

Cincinnati, J. E. M. D. R. P. C. U., H. R. A. E. P. P. C. P. S. University, et al. (2005). Inorganic Polymers, Oxford University Press, USA.

Cordeiro, R. A., N. Rocha, et al. (2013). "Synthesis of well-defined poly(2-(dimethylamino)ethyl methacrylate) under mild conditions and its co-polymers with cholesterol and PEG using Fe(0)/Cu(ii) based SARA ATRP." Polymer Chemistry **4**(10): 3088-3097.

Cosgrove, T. (2010). Colloid Science: Principles, Methods and Applications, Wiley.

Creutz, S. and R. Jérôme (1999). "Effectiveness of Poly(vinylpyridine) Block Copolymers as Stabilizers of Aqueous Titanium Dioxide Dispersions of a High Solid Content." Langmuir **15**(21): 7145-7156.

Creutz, S. and R. Jérôme (2000). "Effectiveness of block copolymers as stabilizers for aqueous titanium dioxide dispersions of a high solid content." Progress in Organic Coatings **40**(1–4): 21-29.

Creutz, S., R. Jerome, et al. (1998). "Design of polymeric dispersants for waterborne coatings." Journal of Coatings Technology **70**(883): 41-46.

Davis, K. A. and K. Matyjaszewski (2000). "Atom Transfer Radical Polymerization of tert-Butyl Acrylate and Preparation of Block Copolymers." Macromolecules **33**(11): 4039-4047.

De Clercq, B., J. Laperre, et al. (2005). "The controlled radical polymerisation process as an instrument for tailor-made coating applications." Progress in Organic Coatings **53**(3): 195-206.

Ebewele, R. O. (2000). Polymer Science and Technology, Taylor & Francis.

Farrokhpay, S. (2009). "A review of polymeric dispersant stabilisation of titania pigment." Advances in Colloid and Interface Science **151**(1-2): 24-32.

Farrokhpay, S., G. E. Morris, et al. (2005). "Influence of polymer functional group architecture on titania pigment dispersion." Colloids and Surfaces A: Physicochemical and Engineering Aspects **253**(1–3): 183-191.

Farrokhpay, S., G. E. Morris, et al. (2010). "Stabilisation of titania pigment particles with anionic polymeric dispersants." Powder Technology **202**(1-3): 143-150.

Hamley, I. W. (2004). Developments in Block Copolymer Science and Technology, Wiley.

Herbst, W. and K. Hunger (2006). Industrial Organic Pigments: Production, Properties, Applications, Wiley.

Karakas, F. and M. S. Celik (2013). "Mechanism of TiO2 stabilization by low molecular weight NaPAA in reference to water-borne paint suspensions." Colloids and Surfaces a-Physicochemical and Engineering Aspects **434**: 185-193.

Kumar, A. and R. K. Gupta (2003). Fundamentals of Polymer Engineering, Revised and Expanded, Taylor & Francis.

Lambourne, R. and T. A. Strivens (1999). Paint and Surface Coatings: Theory and Practice, William Andrew Pub.

Lazzari, M., G. Liu, et al. (2007). Block Copolymers in Nanoscience, John Wiley & Sons.

Mandzy, N., E. Grulke, et al. (2005). "Breakage of TiO2 agglomerates in electrostatically stabilized aqueous dispersions." Powder Technology **160**(2): 121-126.

Martinez-Castro, N., Z. Zhou, et al. (2010). "Preparation and properties of poly(ethylene glycol)-block-poly(acrylic acid)-coated cobalt nanocrystals." Polymer **51**(12): 2629-2635.

Matyjaszewski, K. (2012). "Atom Transfer Radical Polymerization (ATRP): Current Status and Future Perspectives." Macromolecules **45**(10): 4015-4039.

Matyjaszewski, K. and N. V. Tsarevsky (2009). "Nanostructured functional materials prepared by atom transfer radical polymerization." Nat Chem **1**(4): 276-288.

Mueller, L., W. Jakubowski, et al. (2007). "Successful Chain Extension of Polyacrylate and Polystyrene Macroinitiators with Methacrylates in an ARGET and ICAR ATRP." Macromolecules **40**(18): 6464-6472.

Mulder, M. (1996). Basic Principles of Membrane Technology, Springer.

Myers, D. (1991). Surfaces, Interfaces, and Colloids: Principles and Applications, Wiley.

Othman, S. H., S. Abdul Rashid, et al. (2012). "Dispersion and Stabilization of Photocatalytic TiO2 Nanoparticles in Aqueous Suspension for Coatings Applications." Journal of Nanomaterials **2012**: 10.

Qiu, J., B. Charleux, et al. (2001). "Controlled/living radical polymerization in aqueous media: homogeneous and heterogeneous systems." Progress in Polymer Science **26**(10): 2083-2134.

Rocha, N., J. Mendes, et al. (2014). "Poly(ethylene glycol)-block-poly(4-vinyl pyridine) as a versatile block copolymer to prepare nanoaggregates of superparamagnetic iron oxide nanoparticles." Journal of Materials Chemistry B **2**(11): 1565-1575.

Rocha, N., P. Mendonça, et al. (2013). The Importance of Controlled/Living Radical Polymerization Techniques in the Design of Tailor Made Nanoparticles for Drug Delivery Systems. Drug Delivery Systems: Advanced Technologies Potentially Applicable in Personalised Treatment. J. Coelho, Springer Netherlands. **4:** 315-357.

Rocha, N., D. P. Rodrigues, et al. (2014). "Novel nanoaggregates with peripheric superparamagnetic iron oxide nanoparticles and organic cores through self-assembly of tailor-made block copolymers." RSC Advances **4**(47): 24428-24432.

Schmitz, J., H. Frommelius, et al. (1999). "A new concept for dispersing agents in aqueous coatings." Progress in Organic Coatings **35**(1-4): 191-196.

Stevens, M. P. (1999). Polymer Chemistry: An Introduction, Oxford University Press.

Teraoka, I. (2002). Polymer Solutions: An Introduction to Physical Properties, Wiley.

Wang, X., L. Zhao, et al. (2010). "Stability enhancement of ZnTPPS in acidic aqueous solutions by polymeric micelles." Chemical Communications **46**(35): 6560-6562.

Wehrung, J.-F., D. Li, et al. (2013). "Using block copolymers to enhance photosensitized water reduction for hydrogen gas generation." Journal of Materials Chemistry A **1**(29): 8358-8362.

Wei, X., G. Zhu, et al. (2013). "Synthesis, Characterization, and Photocatalysis of Well-Dispersible Phase-Pure Anatase TiO2 Nanoparticles." International Journal of Photoenergy **2013**: 6.

Xiao, J., W. Chen, et al. (2013). "Polymer/TiO2 Hybrid Nanoparticles with Highly Effective UV-Screening but Eliminated Photocatalytic Activity." Macromolecules **46**(2): 375-383.

Yang, H., Y. Su, et al. (2007). "Synthesis of amphiphilic triblock copolymers and application for morphology control of calcium carbonate crystals." Polymer **48**(15): 4344-4351.

Yuan, L., W. Chen, et al. (2012). "PEG-b-PtBA-b-PHEMA well-defined amphiphilic triblock copolymer: Synthesis, self-assembly, and application in drug delivery." Journal of Polymer Science Part A: Polymer Chemistry **50**(21): 4579-4588.

Zhang, W., L. Shi, et al. (2005). "Micellization of Thermo- and pH-Responsive Triblock Copolymer of Poly(ethylene glycol)-b-poly(4-vinylpyridine)-b-poly(N-isopropylacrylamide)." Macromolecules **38**(21): 8850-8852.

Zhang, X., C. Ai, et al. (2011). "Synthesis of zwitterionic shell cross-linked micelles with pH-dependent hydrophilicity." Journal of Colloid and Interface Science **356**(1): 24-30.

Net bibliography

BASF, http://www.basf.com/group/corporate/en/literature-document:

/Sales+Products+Dispex+AA+4040+old+Dispex+A40-Brochure--

Dispersing+Agents+and+Rheology+Modifiers-English.pdf, consulted in 06/09/2014.

Dow Corning, http://www.dowcorning.com/content/publishedlit/

Modern_formulations_for_architectural_paints.pdf, consulted in 06/09/2014.

Appendix

Appendix I

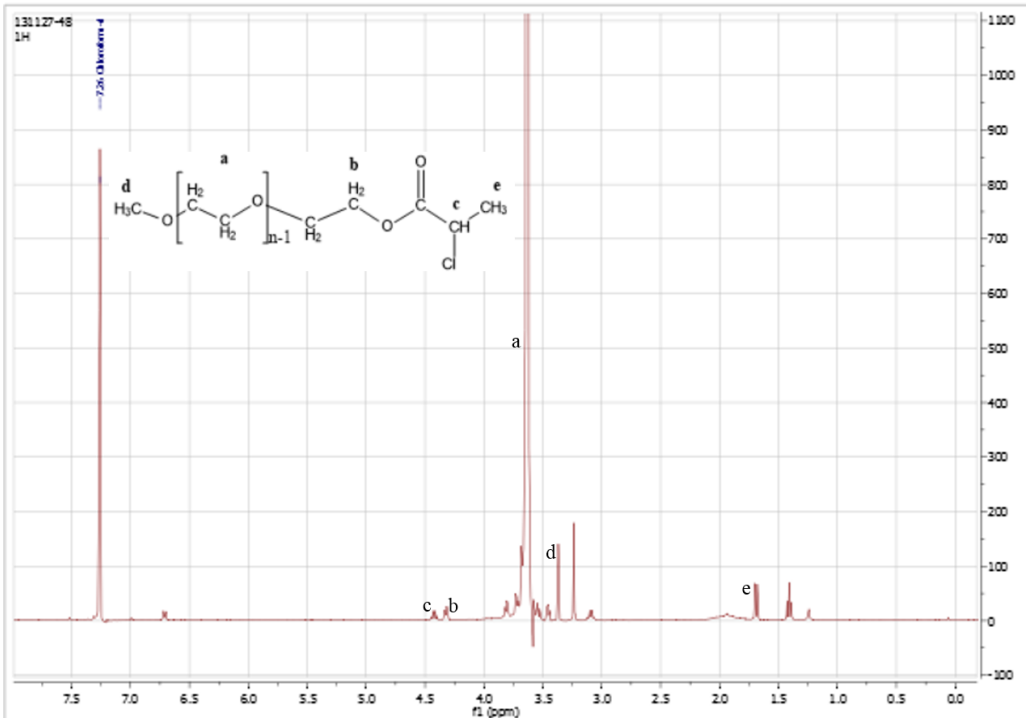

Figure I-1 – ^{1}H-NMR spectra of mPEG-Cl in $CDCl_3$ and molecular structure.

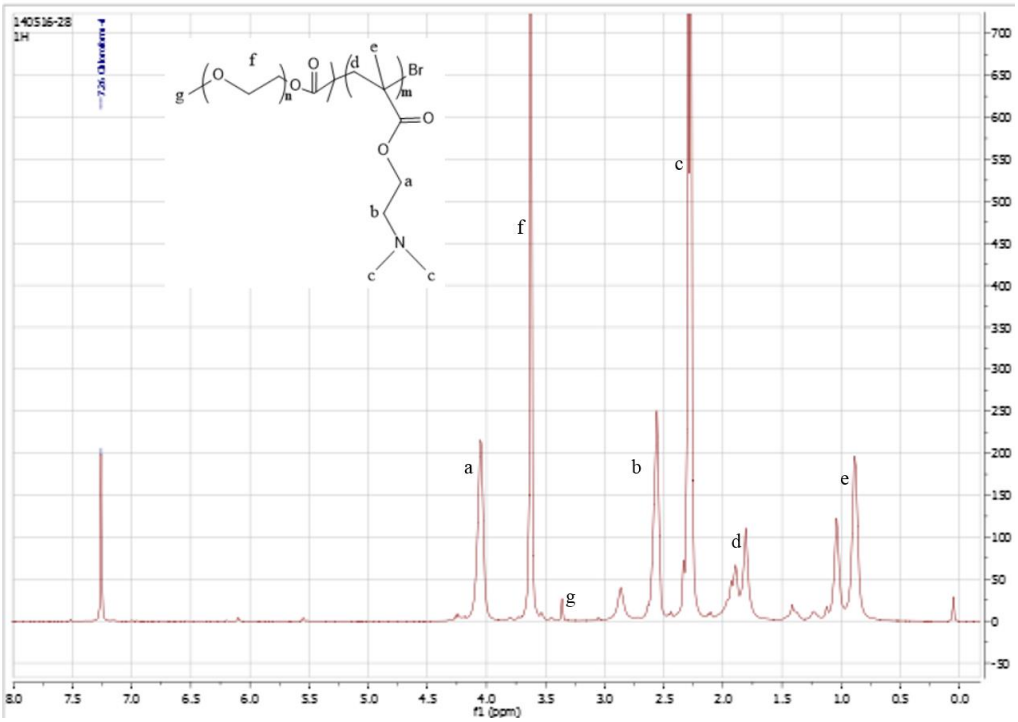

Figure I-2 – ^{1}H-NMR spectra of $mPEG_{45}$-*b*-$PDMAEMA_{38}$ in $CDCl_3$ and molecular structure.

Appendix II

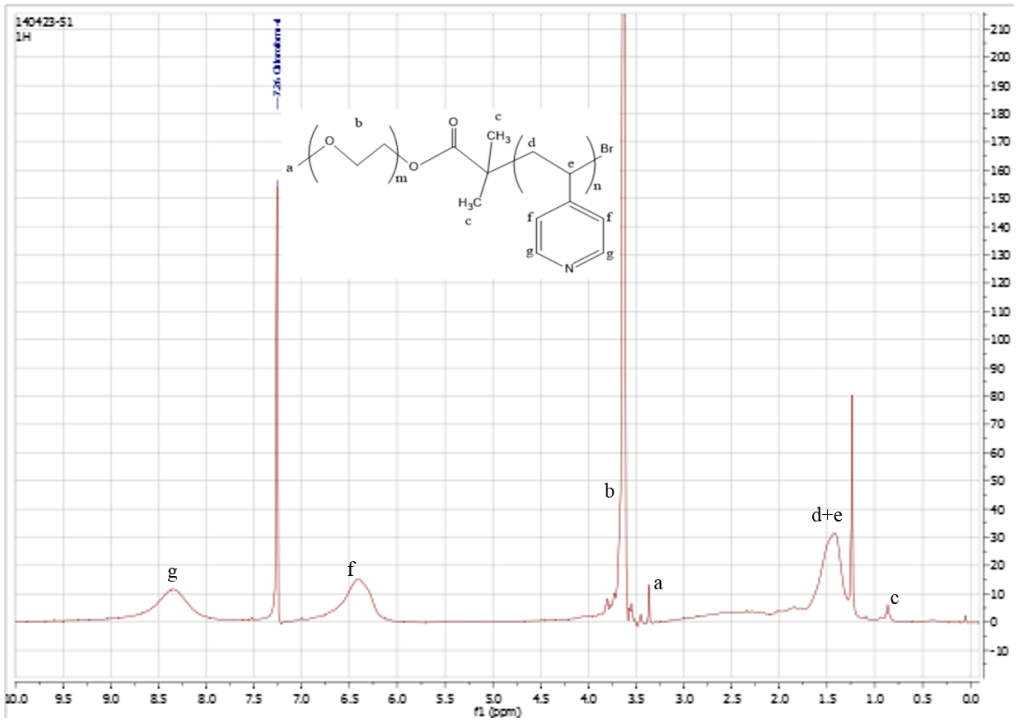

Figure II-1 – ^{1}H-NMR spectra of mPEG$_{113}$-*b*-P4VP$_{55}$ in $CDCl_3$ and molecular structure.

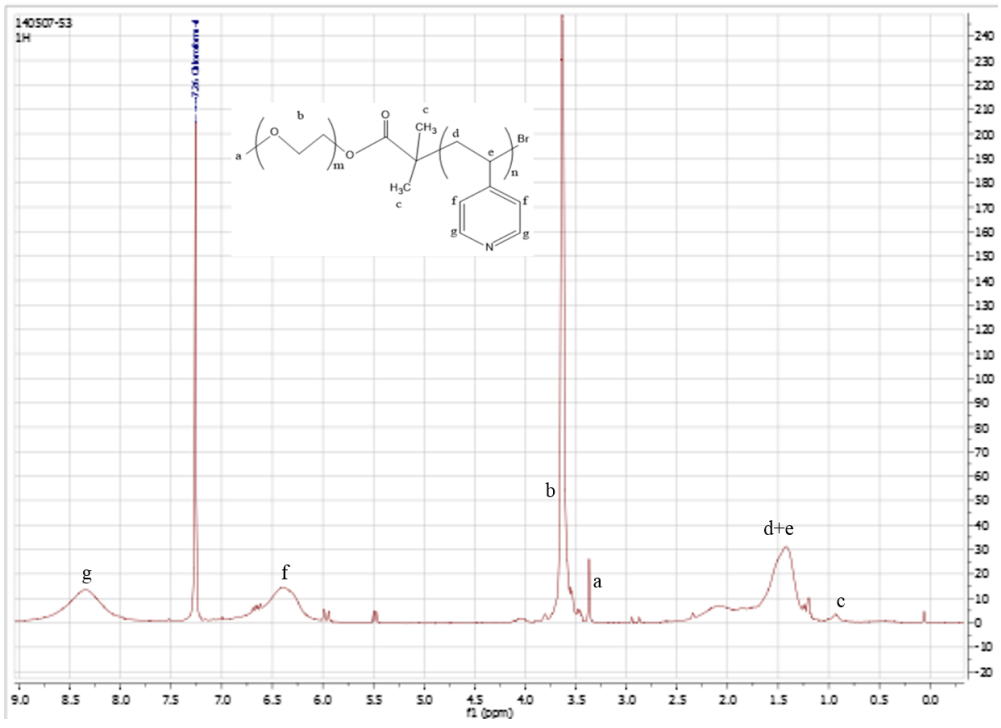

Figure II-2 – ^{1}H-NMR spectra of mPEG$_{45}$-*b*-P4VP$_{31}$ in $CDCl_3$ and molecular structure.

Appendix III

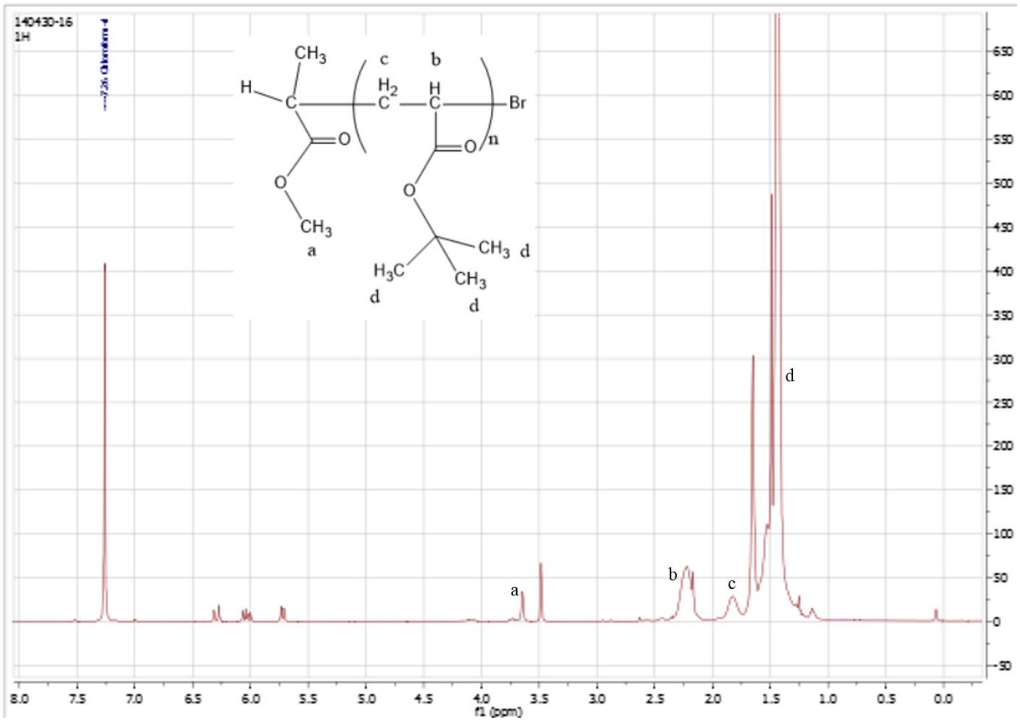

Figure III-1 – ^{1}H-NMR spectra of PtBA in $CDCl_3$ and molecular structure.

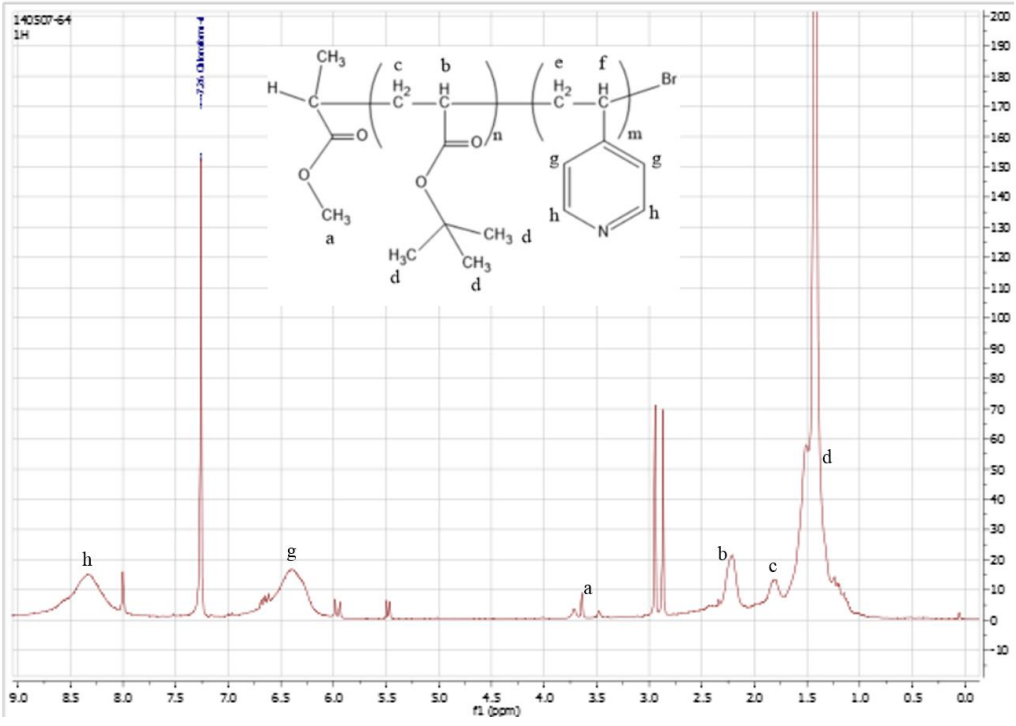

Figure III-2 – ^{1}H-NMR spectra of $PtBA_{37}$-*b*-$P4VP_{30}$ in $CDCl_3$ and molecular structure.

Appendix IV

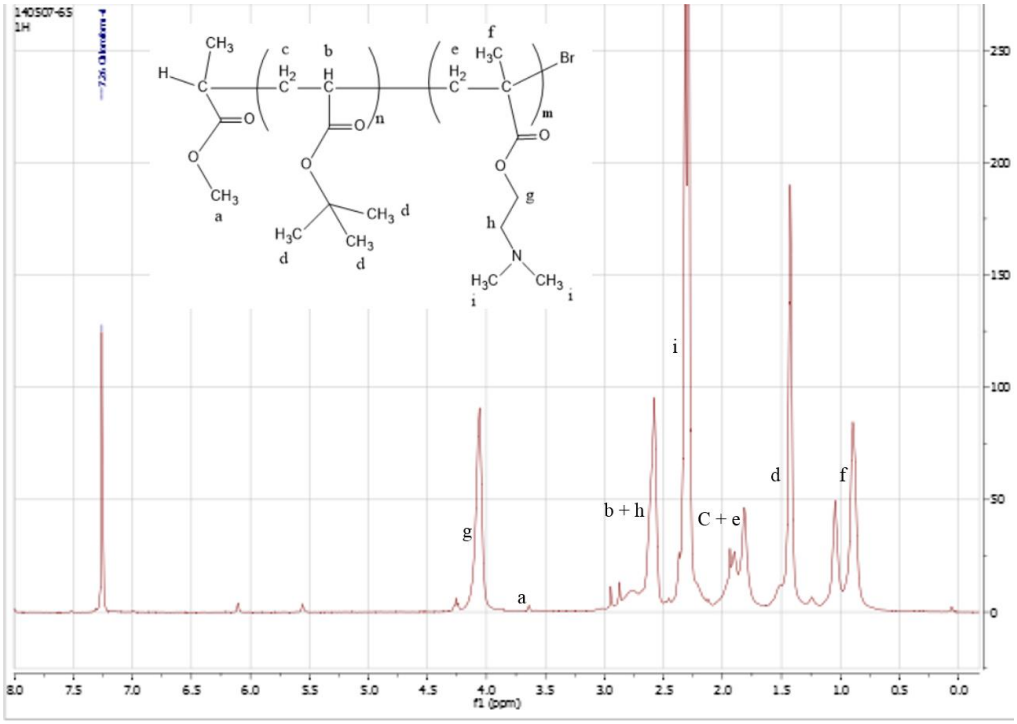

Figure IV-1 – ^{1}H-NMR spectra of PtBA$_{37}$-*b*-PDMAEMA$_{56}$ in $CDCl_3$ and molecular structure.

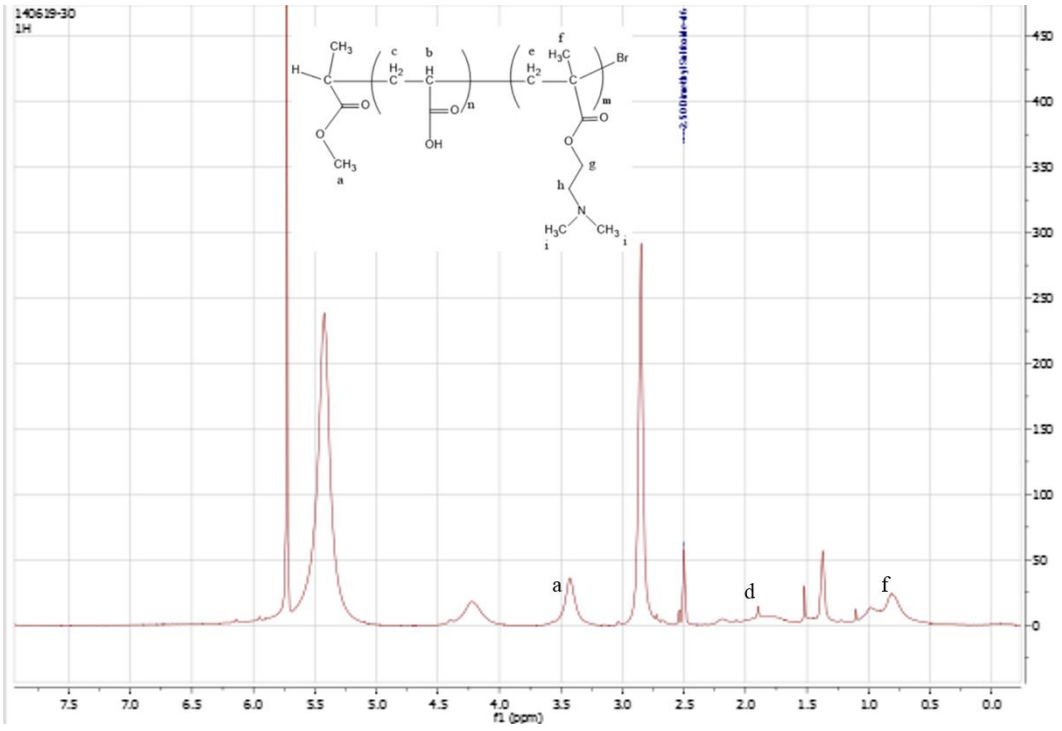

Figure IV-2 – ^{1}H-NMR spectra of PAA$_{37}$-*b*-PDMAEMA$_{56}$ in DMSO and molecular structure.

Appendix V

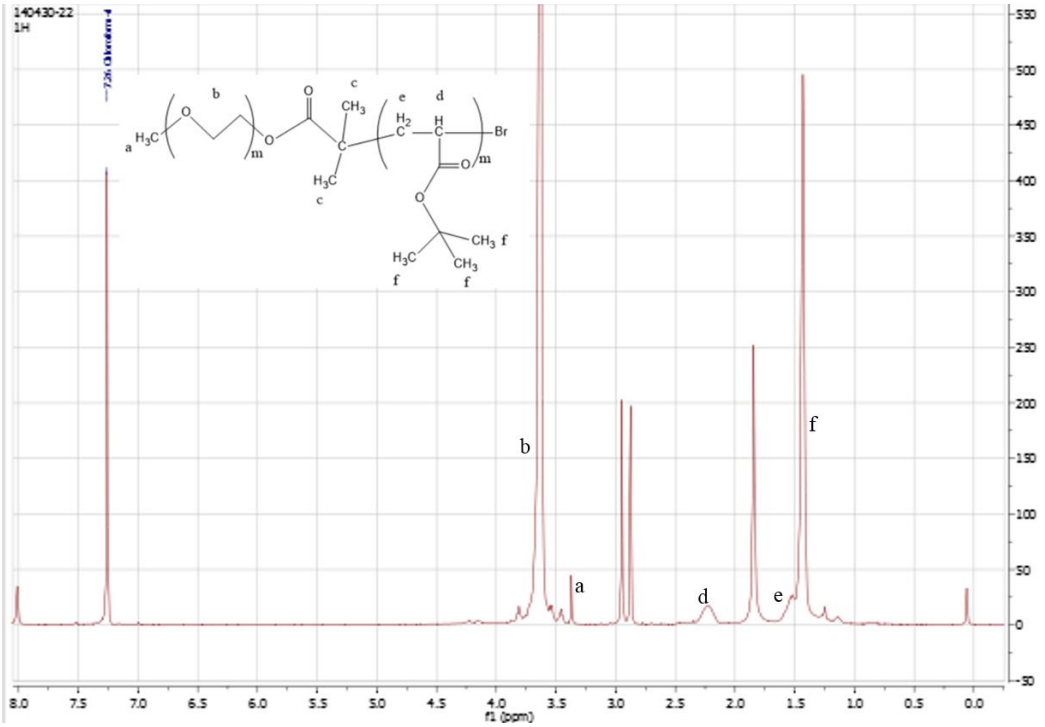

Figure V-1 – ^{1}H-NMR spectra of PEG_{113}-*b*-$PtBA_{12}$ in $CDCl_3$ and molecular structure.

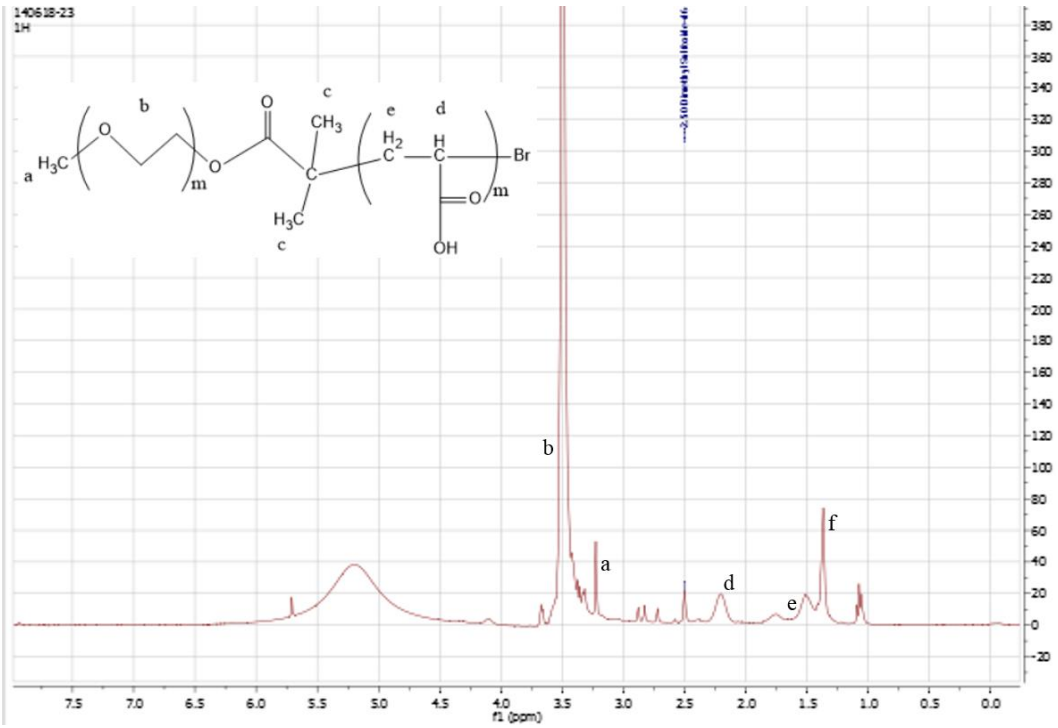

Figure V-2 – ^{1}H-NMR spectra of PEG_{113}-*b*-PAA_{12} in DMSO and molecular structure.

Appendix VI

	Component		Parts
Milling phase	Solvent	Water	17.40
	Thickener	Natrosol 250	0.07
	pH modifier	Sodium Hydroxide (20% w/w solution)	0.02
	Dispersant	Dispex GA40	0.38
	Antifoam	DC 68 Additive	0.55
	Pigment	TiO_2 - TR92	19.72
	Filler	Kaolin - Optimat 2550	4.08
	Filler	Mica - Mica Mkt	5.10
	Filler	Carbital 115 - $CaCO_3$	23.78
Let Down	Thickener	Polyurethane thickener	0.99
	Resin	Acrylic emulsion	26.59
	Coalescing solvent	Dipropylene glycol n-butyl ether	1.11
	Biocide	Acticide MBS	0.22
		Total	100.00

Figure VI-1 – High PVC paint formulation used to assess Dow Corning water resistant additives (Dow Corning, 2014).

Appendix VII

Table VII-1 – Zeta potential and respective deviation values for self-assemble of the copolymers in study in aqueous solution, for several days.

Block Copolymer	Day 0		Day 1		Day 5		Day 6		Day 7		Day 8		Day 9	
	Zeta potential average (mV)	Zeta potential Deviation (mV)	Zeta potential average (mV)	Zeta potential Deviation (mV)	Zeta potential average (mV)	Zeta potential Deviation (mV)	Zeta potential average (mV)	Zeta potential Deviation (mV)	Zeta potential average (mV)	Zeta potential Deviation (mV)	Zeta potential average (mV)	Zeta potential Deviation (mV)	Zeta potential average (mV)	Zeta potential Deviation (mV)
Milli-Q water	-19,4	2,51	-14,7	2,73	-20,3	0,115	-6,46	0,145	-19,4	2,51	-16,5	2,8	-11,2	4,6
$mPEG_{113}$-*b*-$PDMAEMA_{44}$	19,3	0,416	19,2	0,666	23,1	1,37	25,6	3,35	28,6	1,98	26,4	4,09	22,3	3,4
$mPEG_{45}$-*b*-$PDMAEMA_{38}$	18,1	0,751	18,5	1,53	24,3	1,9	24,1	1,42	17,6	1,72	23,7	2,84	22,5	2,41
$mPEG_{113}$-*b*-$P4VP_{55}$	31,6	0,529	31,1	0,306	31	0,611	32	1,07	30,9	0,379	30,8	1,14	30,2	0,252
$mPEG_{45}$-*b*-$P4VP_{31}$	44,5	1,66	40,8	1,39	42,2	3,25	40,4	1,85	40	1,19	40,4	1,22	21,7	6,77
PAA_{26}-*b*-$P4VP_{30}$	57,8	1,06	48,6	0,987	54,3	1,91	52,8	0,862	54,6	1,46	57,4	1,01	57,6	0,306
PAA_{41}-*b*-$PDMAEMA_{56}$	55,4	4,82	53,6	1,33	57,9	2,12	56,6	0,737	50,3	5,56	35,2	4,3	38,1	1,56
$mPEG_{113}$-*b*-$PtBA_{12}$	4,85	0,701	4,29	0,672	4,83	0,924	4,35	0,615	3,62	0,601	4,46	0,591	3,05	1,77
Additol	-47,1	4,45	-21,9	3,26	-6,76	1,01	-6,99	3,4	-5,59	0,643	-5,44	1,62	-4,68	0,429

Appendix VIII

Table VIII-1 – Zeta potential and respective deviation values for self-assemble of the copolymers in study in the presence of TiO_2 particles for several days.

Block Copolymer	Day 0		Day 1		Day 5		Day 6		Day 7		Day 8		Day 9	
	Zeta potential average (mV)	Zeta potential Deviation (mV)	Zeta potential average (mV)	Zeta potential Deviation (mV)	Zeta potential average (mV)	Zeta potential Deviation (mV)	Zeta potential average (mV)	Zeta potential Deviation (mV)	Zeta potential average (mV)	Zeta potential Deviation (mV)	Zeta potential average (mV)	Zeta potential Deviation (mV)	Zeta potential average (mV)	Zeta potential Deviation (mV)
TiO_2	-2,85	1,97	-26,4	1,4	-26,6	1	-23,2	2,01	-22,9	2,05	-20,9	2,95	-18,5	2,02
$mPEG_{113}$-*b*-$PDMAEMA_{44}$	28,5	0,208	28,8	0,265	29,6	0,755	28,9	0,755	28,3	0,153	28,1	0,208	28,3	0,577
$mPEG_{45}$-*b*-$PDMAEMA_{38}$	25,6	0,0577	25,7	0,635	23,9	0,458	25,2	0,1	26	0,252	25,5	0,608	23,6	0,814
$mPEG_{113}$-*b*-$P4VP_{55}$	41,5	0,929	40,3	0,265	39,6	0,721	40,1	0,751	38,6	0,872	39,5	0,252	37,6	0,987
$mPEG_{45}$-*b*-$P4VP_{31}$	44,1	1	43,9	0,872	43,8	0,635	43,8	0,5	43,2	0,862	43,7	0,802	41,2	0,404
PAA_{26}-*b*-$P4VP_{30}$	66,8	1,25	64,6	0,416	62,5	0,569	63,4	0,781	61,9	1,24	62,1	0,794	61,4	0,608
PAA_{41}-*b*-$PDMAEMA_{56}$	56,1	0,819	56,2	0,252	55,3	0,907	56,8	0,458	55	0,777	55,7	0,961	54,9	0,289
$mPEG_{113}$-*b*-$PtBA_{12}$	0,26	2,9	2,21	0,746	3,23	0,61	2,93	0,427	3,46	0,606	3,67	0,11	3,89	1,02
Additol	-74,2	1,87	-70,9	0,656	-67,3	1,83	-73,8	0,814	-68,8	1,39	-69,1	2,11	-66,9	2,36

Appendix IX

Table IX-1 – Evolution of the viscosity in the polymeric aqueous solutions.

Block Copolymer	Viscosity (Pa.s)				
	Day 0	Day 1	Day 3	Day 5	Day 11
$mPEG_{113}$-*b*-$PDMAEMA_{44}$	2,03E-03	1,80E-03	1,80E-03	1,73E-03	1,54E-03
$mPEG_{45}$-*b*-$PDMAEMA_{38}$	1,68E-03	1,71E-03	1,73E-03	1,69E-03	1,47E-03
$mPEG_{113}$-*b*-$P4VP_{55}$	1,97E-03	1,79E-03	2,02E-03	1,83E-03	1,81E-03
$mPEG_{45}$-*b*-$P4VP_{31}$	1,77E-03	1,88E-03	1,81E-03	1,86E-03	1,86E-03
PAA_{26}-*b*-$P4VP_{30}$	1,95E-03	2,23E-03	2,16E-03	1,97E-03	2,16E-03
PAA_{41}-*b*-$PDMAEMA_{56}$	1,98E-03	1,95E-03	1,92E-03	1,92E-03	1,69E-03
$mPEG_{113}$-*b*-$PtBA_{12}$	1,73E-03	1,70E-03	1,67E-03	1,73E-03	1,54E-03
Additol	1,78E-03	1,73E-03	1,70E-03	1,88E-03	1,55E-03
Milli-Q water	1,82E-03	1,74E-03	1,67E-03	1,68E-03	1,54E-03

Table IX-2 – Evolution of the viscosity in the TiO_2 suspensions.

Block Copolymer	Viscosity (Pa.s)				
	Day 0	Day 1	Day 3	Day 5	Day 11
$mPEG_{113}$-*b*-$PDMAEMA_{44}$	2,95E-03	1,55E-03	1,59E-03	1,74E-03	1,88E-03
$mPEG_{45}$-*b*-$PDMAEMA_{38}$	2,62E-03	1,51E-03	1,47E-03	1,66E-03	1,90E-03
$mPEG_{113}$-*b*-$P4VP_{55}$	1,70E-03	1,57E-03	1,48E-03	1,84E-03	1,95E-03
$mPEG_{45}$-*b*-$P4VP_{31}$	1,89E-03	1,69E-03	1,59E-03	1,63E-03	1,87E-03
PAA_{26}-*b*-$P4VP_{30}$	1,66E-03	1,55E-03	1,99E-03	1,85E-03	1,80E-03
PAA_{41}-*b*-$PDMAEMA_{56}$	1,91E-03	1,90E-03	1,89E-03	1,86E-03	2,22E-03
$mPEG_{113}$-*b*-$PtBA_{12}$	1,69E-03	1,73E-03	1,60E-03	1,87E-03	1,93E-03
Additol	1,63E-03	1,69E-03	1,65E-03	1,62E-03	1,87E-03
TiO_2	2,69E-03	1,48E-03	1,56E-03	1,58E-03	1,74E-03

Appendix X

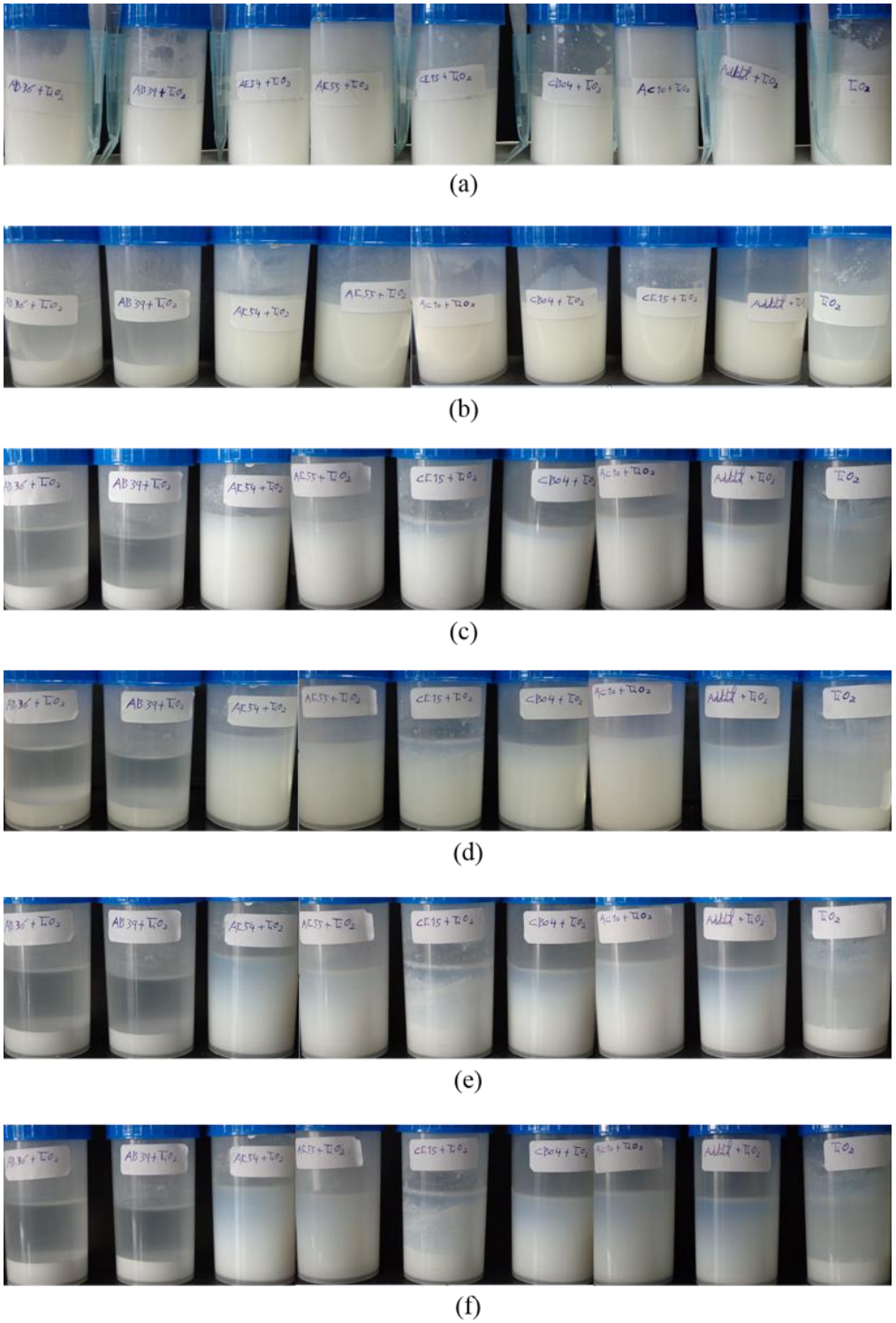

Figure X-1 – Deposition behavior of TiO_2 suspensions with stabilization of different copolymers, for samples of viscosity tests, at different days: (a) initial day of tests, (b) 1st day, (c) 4th day, (d) 6th day, (e) 12th day, (f) 14th day. From the right to the left the samples are: $mPEG_{113}$-*b*-$PDMAEMA_{44}$, $mPEG_{45}$-*b*-$PDMAEMA_{38}$, $mPEG_{113}$-*b*-$P4VP_{55}$, $mPEG_{45}$-*b*-$P4VP_{31}$, PAA_{26}-*b*-$P4VP_{30}$, PAA_{41}-*b*-$PDMAEMA_{56}$, $mPEG_{113}$-*b*-$PtBA_{12}$, Additol VXW 6200, and TiO_2.